

THE HUBBLE CONSTANT: A SUMMARY OF THE HST PROGRAM FOR THE LUMINOSITY CALIBRATION OF TYPE Ia SUPERNOVAE BY MEANS OF CEPHEIDS

A. Sandage

*The Observatories of the Carnegie Institution of Washington,
813 Santa Barbara Street, Pasadena, CA 91101*

G. A. Tammann

*Astronomisches Institut der Universität Basel,
Venusstrasse 7, CH-4102 Binningen, Switzerland*

G-A.Tammann@unibas.ch

A. Saha

NOAO, P.O. Box 26732, Tucson, AZ 85726

saha@noao.edu

B. Reindl

*Astronomisches Institut der Universität Basel,
Venusstrasse 7, CH-4102 Binningen, Switzerland*

reindl@astro.unibas.ch

F. D. Macchetto, N. Panagia

*Space Telescope Science Institut,
3700 San Martin Drive, Baltimore, MD 21218*

macchetto@stsci.edu, panagia@stsci.edu

ABSTRACT

This is the fifth and final summary paper of our 15 year program using the Hubble Space Telescope (HST) to determine the Hubble constant using Type Ia supernovae, calibrated with Cepheid variables in nearby galaxies that hosted them. Several developments not contemplated at the start of the program in

1990 have made it necessary to put the summary on H_0 on a broader basis than originally thought, making four preparatory papers (cited in the text) necessary. The new Cepheid distances of the subset of 10 galaxies, which were hosts of normal SNe Ia, give weighted mean luminosities in B , V , and I at maximum light of -19.49 , -19.46 , and -19.22 , respectively. These calibrate the adopted SNe Ia Hubble diagram from Paper III to give $H_0 = 62.3 \pm 1.3$ (random) ± 5.0 (systematic) in units of $\text{km s}^{-1} \text{Mpc}^{-1}$. This is a global value because it uses the Hubble diagram between redshift limits of 3000 and 20 000 km s^{-1} reduced to the CMB kinematic frame, well beyond the effects of any local random and streaming motions. Local values of H_0 between 4.4 and 30 Mpc from Cepheids, SNe Ia, 21 cm-line widths, and the tip of the red-giant branch (TRGB) all agree within 5% of our global value. This agreement of H_0 on all scales from $\sim 4 - 200$ Mpc finds its most obvious explanation in the smoothing effect of vacuum energy on the otherwise lumpy gravitational field due to the non-uniform distribution of the local galaxies. The physical methods of time delay of gravitational lenses and the Sunyaev-Zeldovich effect are consistent (but with large errors) with our global value. The present result is also not in contradiction with existing analyses of CMB data, because they either lead to wide error margins of H_0 or depend on the choice of unwarranted priors that couple the value of H_0 with a number of otherwise free parameters in the CMB acoustic waves. Our value of H_0 is 14% smaller than the value of H_0 found by Freedman et al. (2001) because our independent Cepheid distances to the six SNe Ia-calibrating galaxies used in that analysis average 0.35 mag larger than those used earlier.

Subject headings: Cepheids — distance scale — galaxies: distances and redshifts — supernovae: general

1. INTRODUCTION

Supernovae of Type Ia (SNe Ia) are uniquely suited for the calibration of the Hubble constant H_0 because they are accessible out to large distances, and as the best standard candles known they are insensitive to selection (Malmquist) bias, which has beset the extragalactic distance scale for so long. An HST program to determine the Hubble constant H_0 using Type Ia supernovae (SNe Ia) as standard candles was therefore mounted in 1990 at the time when HST was launched. The plan was to determine Cepheid distances of nearby galaxies which had produced well observed SNe Ia, and to compare their resulting mean absolute magnitudes with the apparent magnitudes of SNe Ia out to $\sim 30\,000 \text{ km s}^{-1}$ (in the present

context referred to as “distant” SNe Ia). This velocity distance is ideal for the determination of the large-scale value of H_0 (cosmic) because it is large enough that any noise in the Hubble flow due to random velocities and local streaming motions of galaxies is negligible compared with the systematic redshift itself, and on the other hand is small enough that cosmological effects are also negligible (except for small K -corrections, see below).

The program progressed step by step. By 2001 we had published with our collaborators the Cepheid distances of eight SNe Ia-bearing galaxies (for references see Saha et al. 2006, hereafter Paper IV). Four additional Cepheid distances of such galaxies are due to other authors. Thus Cepheid distances are now available for 12 SNe Ia of which, however, two are spectroscopically peculiar.

Yet at least four originally unforeseen developments have made it necessary to put the present summary paper on H_0 on a broader basis, which we have prepared in four preceding papers (Tammann, Sandage, & Reindl 2003, hereafter Paper I; Sandage, Tammann & Reindl 2004, hereafter Paper II; Reindl et al. 2005, hereafter Paper III; and Saha et al. 2006, hereafter Paper IV). The four developments are as follows:

(1) The uniformity of SNe Ia. While some pushed SNe I (Kowal 1968; Barbon et al. 1975; Branch 1977; Branch & Bettis 1978; Tammann 1979, 1982), or particularly SNe Ia (Cadonau et al. 1985; Leibundgut, B. 1988, 1991; Sandage & Tammann 1990; Branch & Tammann 1992) as standard candles with the then available observations, others emphasized their variety (Pskovskii 1967, 1984; Barbon et al. 1973; Frogel et al. 1987). Eventually Phillips (1993) proposed a correlation between the decline rate Δm_{15} (the magnitude change during the first 15 days past B maximum) and the absolute magnitude at maximum. The quantitative correlation became convincing when Hamuy et al. (1996) showed that the magnitude residuals from the Hubble diagram regression (Hubble line) are a function of Δm_{15} . There remained some debate between different authors as to the steepness of the correlation. But this is now understood as the result of different assumptions on the intrinsic color of SNe Ia; the Δm_{15} correction on the magnitudes is therefore quite well controlled (Paper III), but remains purely empirical. It became also increasingly clear that spectroscopically peculiar SNe Ia cannot be used as standard candles. The magnitude of normal SNe Ia after correction for Δm_{15} show a scatter about the Hubble line of $\sigma = 0.15$ mag (including errors of the absorption corrections; the *intrinsic* scatter is demonstrably ≤ 0.11 mag). Without the Δm_{15} correction a scatter of 0.21 mag would be observed which shows – contrary to occasional claims – that even without the Δm_{15} correction SNe Ia are highly competitive standard candles. The Δm_{15} corrections do not only affect the observed magnitude scatter, but also the calibration of H_0 at the level of 5% because the calibrating SNe Ia have systematically smaller Δm_{15} values than the distant SNe Ia. [This is because Cepheids require

galaxies with a young population, and the SNe Ia in such galaxies, i.e. in spirals as contrasted to the ellipticals, tend to have small Δm_{15} as first pointed out by Hamuy et al. (1995)]. – It is self-understood that the calibration of H_0 requires a large sample of uniformly reduced distant SNe Ia; this was compiled in Paper III. The large size of the sample is due to the heroic effort of many observers who have collected the necessary photometry over the years.

(2) The difference of the P - L relation of Cepheids in the Galaxy and in LMC. In Paper I & II it was shown that not only do the Galactic period-color (P - C) relations in $(B-V)$ and $(V-I)$ have different slopes than in the LMC, but – as a necessary consequence – the period-luminosity (P - L) relations in B , V , and I have different slopes, and hence different luminosities at given periods, in the two galaxies. Confirmation, among other indicators, is that the lightcurve shape at a given period differ between Cepheids in the Galaxy and the LMC (Tanvir et al. 2005).

This came as a rather unexpected complication for the determination of Cepheid distances. It requires that the P - L relations of the two galaxies must be based on independent zero-points. An update of the zero-points adopted in Paper II and IV and their errors is given in § 4.3 (2b). The inequality of the P - L relations raises a deep problem: which relation, or an interpolation between them, is to be used for a particular galaxy?

(3) In Paper IV it was decided to determine *two* Cepheid distances for each SNIa host galaxies, once $\mu^0(\text{Gal})$ with the P - L relation of the relatively metal-rich Galactic Cepheids, and once $\mu^0(\text{LMC})$ with the P - L relation of the metal-poor LMC Cepheids, and then to interpolate – and slightly extrapolate – between the two values according to metallicity, expressed by the new $[\text{O}/\text{H}]$ scale of Sakai et al. (2004), hereafter denoted by $[\text{O}/\text{H}]_{\text{Sakai}}$. The resulting moduli μ_Z^0 are in this way corrected for metallicity, provided the full difference between the Galactic and LMC P - L relation is in fact caused by metallicity differences. In Paper II only part of the difference between $\mu^0(\text{Gal})$ and $\mu^0(\text{LMC})$ could be proved to be caused by the line blanketing effect of metal lines, but most of the difference could not be explained. Thus it remained a hypothesis that *all* of the difference is due to metallicity variations.

Perhaps the first to predict that the position of the edges of the Cepheid instability strip is a function of chemical composition (in its effect on the atmospheric opacity) was John Cox (1959; 1980, eq. 10.4). The sense was that the strip boundaries move bluewards with decreasing Z , yet redwards with decreasing Y . Hence, for a particular $\Delta Y/\Delta Z$, if Y increases with increasing Z , there will be compensation in the $L - T_e$ instability line, and the strip boundary is in this case almost independent of variable Y and Z for that value of $\Delta Y/\Delta Z$. Among the first to calculate the effect were Christy (1966), van Albada & Baker (1971), and Tuggle & Iben (1972). Sandage et al. (1999) used the modern models of Chiosi et al. (1992,

1993) to show that the effects of Y and Z nearly compensate when $\Delta Y/\Delta Z \sim 5.5$ (see eq. 50 of Paper II).

The situation has become much clearer due to recent model calculations by Fiorentino et al. (2002) and Marconi et al. (2005) who show that the strip moves bluewards with decreasing Z , irrespective of any reasonable value of Y . The models of Marconi et al. (2005) can match the observed P - L relation of LMC, *including its break at* $\log P = 1$, impressively well, except that the model colors ($V-I$) are still too red by ~ 0.1 mag at the long periods ($\langle \log P \rangle \approx 1.5$) needed for Cepheids outside the Local Group. A corresponding color difference persists for $\langle \log P \rangle = 1.5$ also between the observed and theoretical Galactic P - L relations in V and I . Yet the main point here is that the shift of the instability strip to higher temperatures with decreasing metallicity is no longer a hypothesis, but is predicted by model calculations.

Empirical support for the metallicity corrections comes from comparing the resulting μ_Z^0 of 37 galaxies in Paper IV with independent TRGB distances, as far as available, and with velocity distances. The distances $\mu_Z^0 - \mu_{\text{TRGB}}^0$ and $\mu_Z^0 - \mu_{\text{vel}}^0$ show no significant dependence on $[\text{O}/\text{H}]$. A clear dependence does arise, however, if $\mu^0(\text{Gal})$ or $\mu^0(\text{LMC})$ were used instead of μ_Z^0 . Also the strong metal dependence of the SN Ia luminosities based on $\mu^0(\text{LMC})$ becomes insignificant if μ_Z^0 is used instead (Paper IV).

The ten nearby galaxies with Cepheid distances that have hosted normal SNe Ia carry metallicity corrections, which were found (Paper IV) to depend not only on the metallicity, but also on the mean period of the Cepheids. The corrections vary for $\mu^0(\text{Gal})$ between -0.30 and $+0.10$ mag, and for $\mu^0(\text{LMC})$ between -0.11 and $+0.36$ mag. The *mean* corrections are $\langle \Delta \mu_Z \rangle = -0.02$ for $\mu^0(\text{Gal})$ and $+0.20$ mag for $\mu^0(\text{LMC})$. The small mean correction in case of $\mu^0(\text{Gal})$ is due to the fact that the mean metallicity of $[\text{O}/\text{H}]_{\text{Sakai}} = 8.55$ of the ten calibrating galaxies is close to the metallicity of the Galactic Cepheids (8.60). (The notation $[\text{O}/\text{H}]_{\text{Sakai}}$ is explained in § 2). Therefore, if one is prepared to accept the simplifying premise that the distances of metal-rich Cepheids should be based on the P - L relation of the metal-rich Galactic Cepheids – without any further metallicity correction – one obtains on average a good approximation (to within 0.02 mag or 1% in distance) to the adopted μ_Z^0 of the calibrators, and hence to the mean luminosity of their SNe Ia.

(4) A new photometric zero-point of the HST WFPC2 camera was determined in Paper IV. It affects six of the present calibrators by 0.02 to 0.07 mag depending on the chip and the epoch of observation. The photometric zero-point of the remaining four galaxies was estimated to deviate by not more than 0.05 mag.

The structure of the paper is as follows: The basic data of twelve SNe Ia (of which ten

are normal SNe Ia) and their host galaxies are compiled from Papers III and IV in § 2. The mean absolute magnitudes M_{BVI} at maximum of the normal SNe Ia are derived in § 3. The values M_{BVI} are combined with the Hubble diagram of more distant SNe Ia to yield in § 4 the large-scale value of H_0 and its error. The local value of H_0 within 2000 km s^{-1} is derived from Cepheids, SNe Ia, 21cm-line width and tip of the red-giant branch (TRGB) distances in § 5. The evidence for H_0 from physical distance determinations is briefly discussed in § 6. In § 7 the conclusions are given.

2. THE BASIC DATA OF THE CALIBRATING SNe Ia AND OF THEIR HOST GALAXIES

The relevant parameters of the 12 galaxies with SNe Ia and known Cepheid distances are compiled in Table 1 from Paper IV (Table A1). Columns (3) and (4) of Table 1 list their recession velocities, corrected to the barycenter of the Local Group (Yahil et al. 1977) and for a self-consistent Virgocentric infall model with a local infall vector of 220 km s^{-1} (Yahil et al. 1980; Tammann & Sandage 1985; Kraan-Korteweg 1986). The metallicities $[\text{O}/\text{H}]_{\text{old}}$ from Kennicutt et al. (1998) and others, as compiled by Ferrarese et al. (2000) are in column (5). The metallicities $[\text{O}/\text{H}]_{\text{Sakai}}$ in column (6) are the T_e -based values introduced by Sakai et al. (2004) and used in Paper IV. In this system Cepheids in the Galaxy have $[\text{O}/\text{H}] = 8.6$ (Andrievsky et al. 2002) on average, and those in LMC 8.34 (Sakai et al. 2004). Column (7) gives the number of Cepheids which enter the various distance determinations. The mean period of the accepted Cepheids is in column (8). Columns (9)-(13) give the distance moduli derived in Paper IV from different P - L relations as follows:

(1) The distance moduli $\mu^0(\text{Gal})$ in column (9) are derived from the *Galactic* P - L relation (derived in Paper I and slightly revised in Paper II) *without* any metallicity correction; their zero-point rests on the Pleiades at $\mu^0 = 5.61$ and with equal weight on moving-atmosphere parallaxes [the Baade-Becker-Wesselink (BBW) method].

(2) The distance moduli $\mu^0(\text{LMC})$ in column (10) are derived from the LMC P - L relations (derived in Paper II) again *without* any metallicity correction; their zero-point rests on LMC at $\mu^0 = 18.54$, as justified in § 4.3, but *excluding* all solutions based on any P - L relations.

(3) The distance moduli $\mu_Z^0(\text{M/F})$ in column (11) are based on the slopes of the old P - L relations of Madore & Freedman (1991), adjusted to a zero-point at $\mu_{\text{LMC}}^0 = 18.54$, and with the *period-independent* metallicity corrections from Paper IV (Table 7, col. [6]); they correspond to $\Delta\mu_Z = -0.65\Delta[\text{O}/\text{H}]_{\text{Sakai}}$. [It was explained in Paper IV why these corrections

are larger for the *long-period* Cepheids under consideration than in Sakai et al. (2004) who give $\Delta\mu_Z = -0.24\Delta[\text{O}/\text{H}]_{\text{old}}$ or $-0.32\Delta[\text{O}/\text{H}]_{\text{Sakai}}$ based on Cepheids with all periods].

(4) The adopted distance moduli μ_Z^0 in column (12) (and their errors in col. [13]) are taken from Paper IV. They are a compromise between items (1) and (2). The method is based on the assumption – now confirmed by Fiorentino et al. (2002) and Marconi et al. (2005), as mentioned before – that their modulus difference is a function of the metallicity *and* of the mean period as expressed in equation (10) in Paper IV.

In Table 2 the relevant parameters of the 12 SNeIa of the sample are compiled from Paper III. Column (2) lists the decline rates Δm_{15} , column (3) the Galactic color excess $E(B-V)_{\text{Gal}}$ from Schlegel et al. (1998), and column (4) the color excess $E(B-V)_{\text{host}}$ in the host galaxy. For the Galactic absorption A_{BVI} conventional absorption-to-reddening ratios 4.1, 3.1, and 1.8, respectively, were assumed, while the corresponding values of 3.65, 2.65, and 1.35 were derived in Paper III for the absorption of the SNeIa in the host galaxies. Columns (5) and (6) give the dereddened pseudo-colors ($B_{\text{max}} - V_{\text{max}}$) and ($V_{\text{max}} - I_{\text{max}}$).¹ The apparent magnitudes m_{BVI}^{corr} (and their adopted errors in parentheses in units of 0.01 mag; formal errors of < 0.05 mag are unrealistic because of the correction for absorption in the host galaxy; they are set to 0.05 mag.) in columns (7)-(9) are corrected for Galactic and host absorption and reduced to a common decline rate of $\Delta m_{15} = 1.1$ and to a common color of $(B-V)_{\text{max}} = -0.024$ [equation (23) in Paper III].

The apparent magnitudes m_{BVI}^{corr} of the calibrating SNeIa in Table 2 are combined with the various distance moduli in Table 1 to yield the absolute magnitudes M_{BVI} in Table 3. Also shown in each column are the straight and weighted mean values of M_{BVI} for the ten normal SNeIa. The two spectroscopically peculiar type Ia supernovae SN 1991T, which is the prototype of an overluminous class, and 1999by which belongs to the underluminous class of SN 1991bg (Paper III) are listed separately; they are not further used in this paper.

3. THE ABSOLUTE MAGNITUDE OF SNeIa

3.1. The Range of Absolute Magnitudes

The mean absolute magnitudes M_{BV} of the ten calibrating SNeIa in Table 3 vary between -19.30 and -19.55 , the M_I values vary between -18.99 and -19.22 . These ranges

¹For brevity we write in this paper $(B-V) \equiv (B_{\text{max}} - V_{\text{max}})$ and $(V-I) \equiv (V_{\text{max}} - I_{\text{max}})$. The values $(B-V)$ and $(V-I)$ are corrected for Galactic and internal reddening. The designations $(B-V)^{\text{corr}}$ and $(V-I)^{\text{corr}}$ mean that the colors are normalized in addition to a decline rate of $\Delta m_{15} = 1.1$.

translate into a variation of H_0 of 10 – 15%. A careful scrutiny of the best values of M_{BVI} is therefore still necessary.

3.2. The Adopted Absolute Magnitudes

The faintest magnitudes in Table 3 come from the distances $\mu^0(\text{LMC})$ which are based on the LMC P - L relations from Paper II. They are *uncorrected* for metallicity as stated before. This is quite unrealistic because the mean metallicity of the calibrating Cepheids ($\langle[\text{O}/\text{H}]_{\text{old}}\rangle = 8.79$, $\langle[\text{O}/\text{H}]_{\text{Sakai}}\rangle = 8.55$) is significantly higher than that of LMC ($[\text{O}/\text{H}]_{\text{old}} = 8.50$, $[\text{O}/\text{H}]_{\text{Sakai}} = 8.34$). If one applies conservatively the period-independent metallicity correction of Sakai et al. (2004), i.e. $\Delta\mu_Z = -0.24([\text{O}/\text{H}]_{\text{old}} - 8.50)$, the metallicity-corrected $\mu_Z^0(\text{LMC})$ become larger by 0.07 mag *on average*. The resulting *weighted* absolute SN magnitudes M_{BVI} are shown in Table 4, line 2. The corresponding average metallicity correction to the $\mu^0(\text{Gal})$, and hence to the M_{BVI} , from the Galactic P - L relation remains at the level of ~ 0.02 mag (to become fainter in B and V), because the mean metallicity of the calibrators is almost as high as that of the Galaxy.

The weighted absolute magnitudes M_{BVI} for the four different solutions in Table 3 take now the values shown in Table 4. The maximum difference within each column of Table 4 is 0.15 mag. However, it must be noted that solution (2) has the lowest weight, because it combines the P - L relations of the metal-poor LMC with the calibrating galaxies whose average metallicity is much closer to the Galactic value. Eliminating therefore solution (2) reduces the difference in each column to an almost negligible value of ≤ 0.03 mag. One could therefore argue for the mean magnitudes of the three solutions. Yet for obvious reasons discussed in great detail in Paper IV we adopt the weighted magnitudes M_{BVI} of solution (4), where the period-dependent metallicity corrections are applied. (It may seem surprising that the adopted magnitudes in Table 4 are almost as bright or in the case of I even brighter than those from the Galactic P - L relation, although the Galactic Cepheids are slightly more metal-rich than the mean value of the calibrating galaxies ($\Delta[\text{O}/\text{H}]_{\text{Sakai}} = 0.05$) and should give – with no metallicity correction applied – somewhat brighter SN Ia magnitudes. However, the exact differences in M_{BVI} in Table 4 are modified by the weighting of individual SNe Ia. Moreover, the only six calibrating SNe Ia with I magnitudes happen to lie in relatively metal-rich galaxies).

3.3. Tests of the Adopted Absolute Magnitudes

In order to test whether the 10 calibrating SNe Ia form a random statistical sample a bootstrap analysis is applied to their M_V magnitudes from Table 3, column (12). A sample of 10 randomly chosen SNe Ia is formed from the list of 10, allowing each SN to occur as many times as it is drawn, and the mean value $\langle M_V \rangle$ is determined. This process is repeated m times; we have chosen $m = 5000$. The distribution of the resulting mean magnitudes is shown in Figure 1. The very good Gaussian fit to the observed distribution argues for the SNe Ia magnitudes being randomly distributed about a mean value. The mean value $M_V = -19.50$ is identical to the unweighted mean in Table 3, column (12).

It is not meaningful to compare the present calibration of $M_V = -19.50$ (unweighted) or -19.46 (weighted) with previous authors, because different authors have used different precepts concerning intrinsic color, color excess, and absorption-to-reddening ratio \mathcal{R} ; some of the published values are also normalized to different values of the decline rate Δm_{15} and the intrinsic color $(B-V)^0$. Since these precepts have little effect on H_0 as long as they are consistently applied to the nearby calibrating SNe Ia and those defining the Hubble diagram, it is more realistic to compare the values of H_0 from different authors. This is done in § 4.4.

To further ensure the homogeneity of the SN sample, their magnitudes M_V are plotted against various parameters in Figure 2. This is to ascertain that the individual magnitudes do or do not depend on age of the photometry, distance, metallicity, mean period of the Cepheids, or decline rate Δm_{15} , nor on the derived parameters like color excess or intrinsic color. As can be seen in Figure 2 there are no significant trends, with the only exception of the weighted solution of M_V versus $[\text{O}/\text{H}]_{\text{Sakai}}$, which suggests a correlation at only the 1.3σ level. We take the magnitude difference of 0.08 ± 0.15 mag (unweighted) or 0.13 ± 0.09 mag (weighted) between the five SNe Ia in metal-poor galaxies and their counterparts in metal-rich galaxies as insignificant, because it depends entirely on the assigned weights. It would therefore be arbitrary to exclude one or more SNe Ia from the sample on the basis of any of the parameters considered.

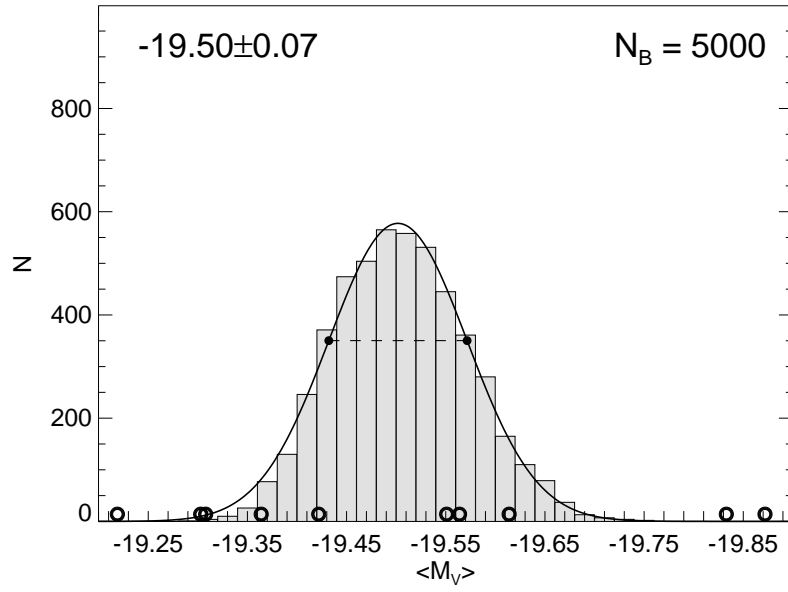


Fig. 1.— A bootstrap analysis of the adopted absolute SN magnitudes M_V . The individual SNe Ia are shown as open circles.

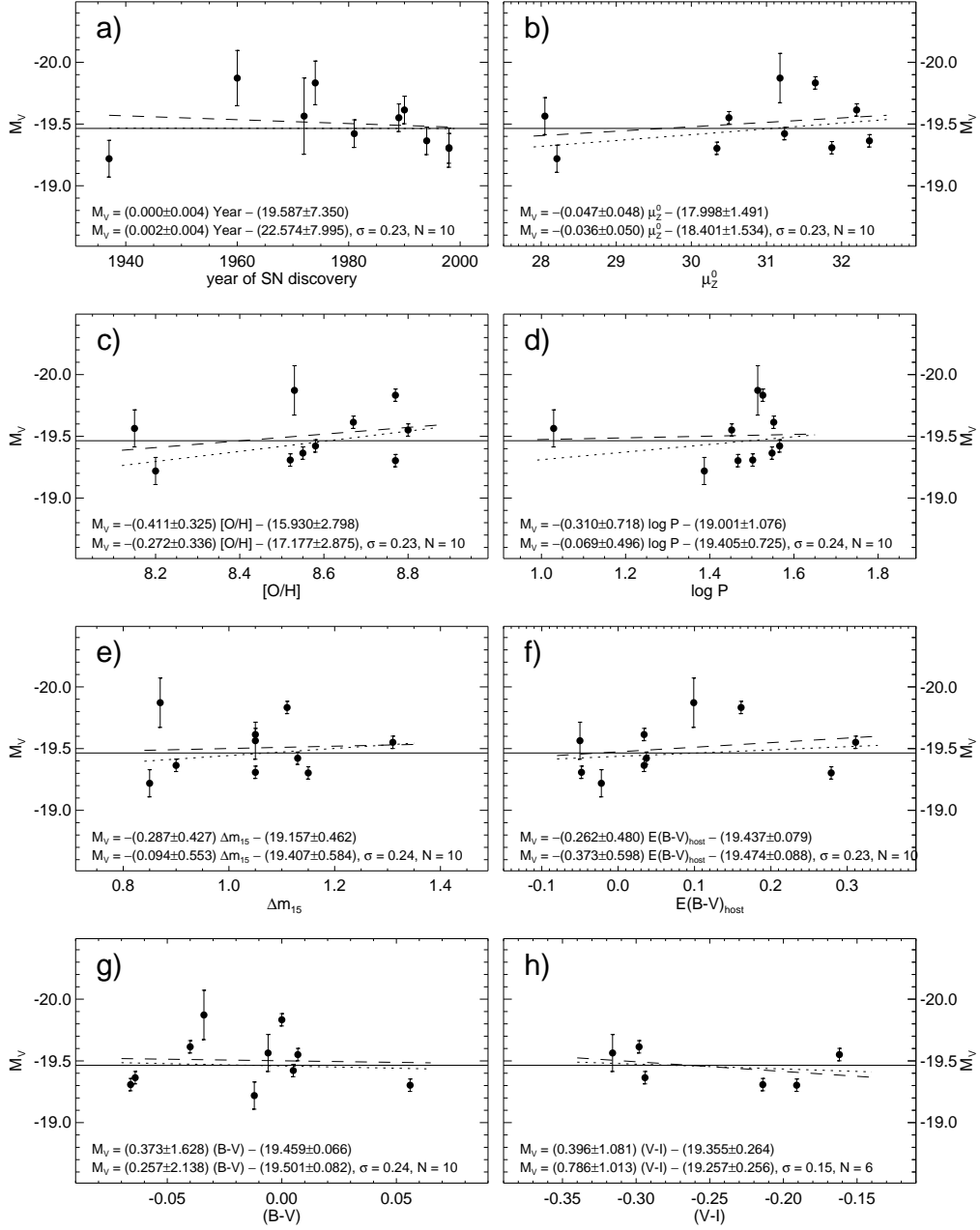


Fig. 2.— The correlation of the absolute SN magnitudes M_V on a) year of discovery, b) distance modulus μ_Z^0 , c) metallicity $[O/H]_{\text{Sakai}}$, d) mean period of the Cepheids $\langle \log P \rangle$, e) the decline rate Δm_{15} , f) the color excess in the host galaxy, g) the intrinsic color $(B-V)$, and h) the intrinsic color $(V-I)$. The upper equation in each panel gives the weighted regression (dotted line), the lower equation the unweighted regression (dashed line).

4. THE LARGE-SCALE VALUE OF H_0

The value of $H_0(\text{cosmic})$ is obtained by combining the intercept C_λ of the Hubble line defined by distant SNeIa with the mean absolute magnitude of the ten calibrating SNeIa. This is because the three parameters are connected by (see Paper III):

$$\log H_0 = 0.2M_\lambda^{\text{corr}} + C_\lambda + 5, \quad (1)$$

where the magnitudes are corrected for the Galactic and internal absorption, reduced to a common decline rate $\Delta m_{15} = 1.1$ and to a common color $(B - V) = -0.024$ at $\Delta m_{15} = 1.1$.

4.1. The Adopted Value of $H_0(\text{cosmic})$

The Hubble diagram for a $\Omega_M = 0.3$, $\Omega_\Lambda = 0.7$ model, using the apparent magnitudes m_V^{corr} of 62 normal SNeIa with $3000 < v_{\text{cmb}} < 20\,000 \text{ km s}^{-1}$, is shown in Figure 3 from the data in Paper III. SNeIa with $v < 3000 \text{ km s}^{-1}$ are not considered because of the possible effect of local random and streaming motions. Also the six SNeIa with $20\,000 < v_{\text{cmb}} \lesssim 30\,000 \text{ km s}^{-1}$ are not used for the solution in order to avoid large K -corrections; if they had been included they would decrease H_0 by less than 1%. Finally five possibly non-normal SNeIa, discussed in Paper III, are excluded from the solution. They are shown as crosses in Figure 3.

With these precepts one obtains for C_B , and correspondingly for C_V and C_I :

$$C_B = 0.693 (N = 62), \quad C_V = 0.688 (N = 62), \quad C_I = 0.637 (N = 58). \quad (2)$$

The random error of the mean is in all three cases as small as 0.004. Inserting these values together with the adopted magnitudes M_{BVI} in Table 4 yields

$$H_0(B) = 62.4 \pm 1.2, \quad H_0(V) = 62.5 \pm 1.2, \quad H_0(I) = 62.1 \pm 1.4,^2 \quad (3)$$

from which we adopt

$$H_0(\text{cosmic}) = 62.3 \pm 1.3. \quad (4)$$

²The units of H_0 are $\text{km s}^{-1} \text{ Mpc}^{-1}$ throughout

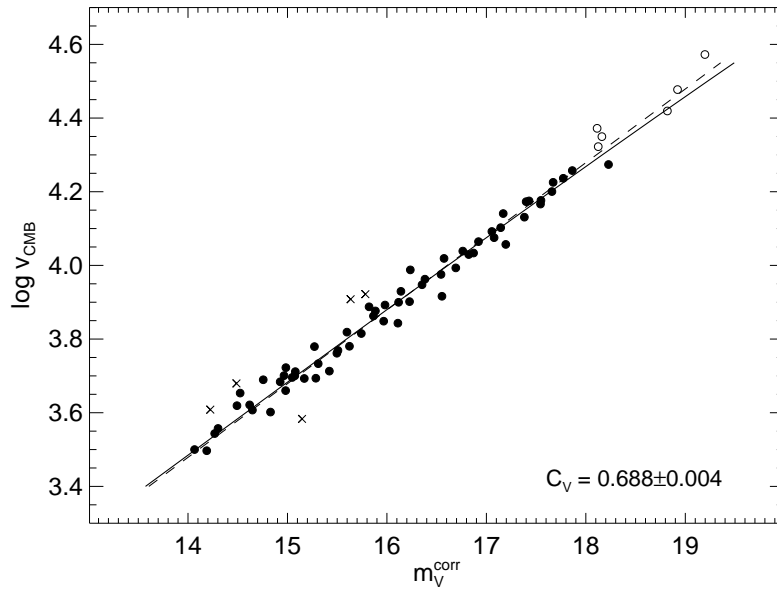


Fig. 3.— The Hubble diagram of 62 normal SNe Ia with $3000 < v_{\text{cmb}} \lesssim 30\,000 \text{ km s}^{-1}$. SNe Ia with $v_{\text{cmb}} > 20\,000 \text{ km s}^{-1}$ are shown as open symbols. Five possibly non-normal SNe Ia are shown as crosses. The dispersion is $\sigma = 0.14 \text{ mag}$. The dashed line holds for a $\Omega_M = 1$ model. The data are from Paper III of Reindl et al. (2005).

An estimate of the systematic error follows in § 4.3. The close agreement of H_0 in all three colors speaks in favor of the *consistent* absorption corrections applied to the calibrators and distant SNe Ia in Paper III. This is also seen in Table 5, where the mean intrinsic colors (after correction for Galactic and internal reddening) of the two sets of SNe Ia are compared. Their agreement is as good as can be expected.

The color agreement between calibrators and distant SNe Ia is of greatest importance. If it had not been the case it would have implied that one set of SNe Ia had systematically larger absorption corrections than the other. A biased value of H_0 would be the result. Other intrinsic colors and hence absorption corrections have been adopted by previous authors. This is unsequential for H_0 as long as the absorption corrections are consistent. But it precludes a comparison of the present values of C_λ with previous authors.

4.2. $H_0(\text{cosmic})$ from a Restricted Sample of SNe Ia

As mentioned before the mean decline rate Δm_{15} of the calibrators is for good reasons smaller than that of the distant SNe Ia (see also Table 5). The value of H_0 depends therefore somewhat on the adopted Δm_{15} corrections. Although the former disagreement between the corrections by different authors are now essentially understood (Paper III), it is interesting to see the effect on H_0 if the distant SNe Ia with $\Delta m_{15} > 1.28$ are omitted. In that case the remaining 40 distant SNe Ia have exactly the same $\langle \Delta m_{15} \rangle$ as the calibrators. They yield $C_V = 0.687 \pm 0.005$ and hence $H_0(V) = 62.4 \pm 1.2$.

An alternative sample restriction is to dispense with the Δm_{15} corrections altogether and to require – since the SNIa luminosity is also a function of the type T of the parent galaxy (as defined in Paper III; see Fig. 10 there) – the mean type T of the parent galaxies be the same for the calibrators and distant galaxies. Omitting the early-type galaxies with $T \leq 1$ leaves a sample of 29 SNe Ia with $\langle T \rangle = 3.9$. Their Hubble diagram gives an intercept of $C_V = 0.694 \pm 0.008$, from which follows $H_0(V) = 63.4 \pm 1.3$. The statistical error is here somewhat larger, because the SNIa luminosity does not correlate as tightly with T as with Δm_{15} , but the essential point is that even without the Δm_{15} corrections H_0 does not change significantly.

4.3. Systematic Errors of H_0

The very small statistical error of $H_0(\text{cosmic})$ in equation (4) is treacherous in view of possible systematic errors. In principle it is not possible to give a reliable estimate of

systematic errors because they are due to the unknown. But one can list points where one depends on assumptions and where random errors of correction factors perpetuate as systematic errors.

The value of H_0 and its systematic error depends on two parameters, i.e. the intercept C_{BVI} of the Hubble diagram of SNeIa and the absolute magnitude M_{BVI} of the calibrating SNeIa. The systematic errors of these two parameters will be discussed in turn.

The intercept C_{BVI} depends on the recession velocities v and on the apparent maximum magnitudes m_{BVI} of SNeIa with $3000 < v < 20\,000 \text{ km s}^{-1}$. Systematic errors of the observed velocities and of their correction to the CMB frame are negligible. Equally the observed apparent magnitudes do not introduce a systematic error. The magnitudes are corrected for Galactic and internal absorption. The internal absorption is based on the intrinsic colors $(B-V)$ and $(V-I)$ of SNeIa at B maximum and 35 days thereafter and on reddening-absorption ratios \mathcal{R}_{BVI} specifically derived for SNeIa (Paper III). These absorption corrections – which remove any dependence of C_{BVI} on galaxy type or on the size of the absorption (Paper III, Table 8, solutions 6-8) – do not introduce a systematic error as long as they are consistently applied to the Hubble diagram SNeIa and to the nearby calibrating SNeIa. The same holds for the normalization of the magnitudes to a decline rate of $\Delta m_{15} = 1.1$ and a color of $(B-V)^{\text{corr}} = -0.024$ (Paper III, equation 23). Therefore the value of the intercept C_{BVI} as such does not introduce a systematic error.

The absolute magnitudes M_{BVI} of the calibrating SNeIa may carry systematic errors for two reasons: (1) errors of their apparent magnitudes due to inconsistencies of their absorption correction and of their normalization to $\Delta m_{15} = 1.1$ and $(B-V)^{\text{corr}} = -0.024$, and (2) metallicity-related distance errors and a zero-point error of the adopted distance scale.

1)a. While the apparent maximum magnitudes of the distant SNeIa are based on CCD photometry, four of the oldest calibrators have photographic photometry, but the magnitudes were transformed into the standard B, V system for SN 1937C [Schaefer 1996a; following this source we have discarded the fainter photometry of Pierce & Jacoby (1995). If it were included here the mean luminosity of the 10 calibrators would decrease by only $\lesssim 0.01 \text{ mag}$], 1960F (Tsvetkov 1983; Schaefer 1996b; Saha et al. 1996b), 1974G (Schaefer 1998), and 1981B (Schaefer 1995). The photoelectric U, B, V photometry (Ardeberg & de Groot 1973) of the bright and far outlying SN 1972 is not affected by background light of the parent galaxy NGC 5253 and is reliable.

The template-fitted lightcurve parameters of these five SNeIa have been compiled in Paper III. They have somewhat larger random errors than later SNeIa and are given corre-

spondingly lower weights, but there is no reason why they should introduce any *systematic* error. Figure 2 shows that their absolute magnitudes are randomly distributed in comparison to later SNe Ia as to the year of discovery, distance, reddening etc. It would be arbitrary to leave out the older SNe Ia. In any case it would make little difference (see 4.4.2).

b. The absorption corrections of the nearby and distant SNe Ia are the product of the consistently derived color excesses $E(B-V)$ and the absorption factor \mathcal{R}_{BVI} . Since there is a mean color excess difference between the two groups of SNe Ia of $\Delta\langle E(B-V)\rangle = 0.027$ (Table 5), an error of the adopted \mathcal{R}_{BVI} of as much as ± 0.5 will cause a systematic error of the absorption A_{BVI} , and hence of the absorption-corrected magnitudes of only 0.014 mag. (Note that variations of \mathcal{R}_{BVI} from galaxy to galaxy are expected to average out in first approximation for samples with ~ 10 and more elements).

c. In analogy to b. an error of the slope a of the $M_{BVI} - \Delta m_{15}$ relation will introduce a systematic error. The mean value of Δm_{15} of the calibrators and distant SNe Ia differs by $\delta\Delta m_{15} = 0.17$ (Table 5). If a has a 10% error of ~ 0.2 (see Paper III, Table 5) the resulting systematic error will remain within 0.04 mag.

d. The normalization of the SNe Ia magnitudes to a common color (Paper III, equation 23) will not introduce an additional systematic error because the calibrators and distant SNe Ia have identical mean $(B-V)$ colors (Table 5).

2)a. The present metallicity corrections $\Delta\mu_Z$, as defined in equation (10) of Paper IV, were derived on purely empirical grounds. They rest on two hypotheses: (1) The observed difference of the $P-L$ relations in the Galaxy and LMC is caused by the metal difference of the two galaxies, and (2) the slopes of the $P-L$ relations transform smoothly from LMC to the Galaxy as $[O/H]$ (or Z) increases. Both points are consistent with earlier models cited in § 1, but it remained the concern that the increase of Y accompanying any increase of Z would counterbalance the shift. Only recent models by Fiorentino et al. (2002) and Marconi et al. (2005) show that the effect of changing Y is small, and the Cepheids become progressively cooler at $L = \text{const}$ as Z increases over a wide range of $\Delta Y/\Delta Z$. Thus our basic assumption as to why the Galactic $P-L$ relations differ from those of LMC is justified by theory.

The observed $P-L$ relations in V and I of the Galaxy yield *larger* distances for long-period Cepheids with $\log P \gtrsim 1.0$ than the observed LMC $P-L$ relations (Paper IV, Fig. 8). Therefore the metallicity corrections $\Delta\mu_Z$ must be positive as the metallicity increases. The models of Marconi et al. (2005) give positive values of $\Delta\mu_Z$ only for very high metallicities of $Z \gtrsim 0.03$, but quantitative agreement cannot be expected since $\Delta\mu_Z$ and its sign depend on the subtle interplay of the slopes in V and I of the Galactic and LMC $P-L$ relations,

which in turn depend on the ridge lines of Cepheids in the $\log L - \log T_e$ plane and which do not necessarily coincide with the mid-line of the instability strip because the evolutionary crossing times during the second crossing of the strip are a strong function of temperature (Alibert et al. 1999).

The mean metallicity of the Cepheids in the ten calibrating galaxies is smaller by only $\Delta[\text{O}/\text{H}]_{\text{Sakai}} = 0.05$ than the adopted metallicity of the Galactic Cepheids. It follows from the models of Marconi et al. (2005) that in this case the Galactic P - L relations are a much better approximation than those of LMC. In fact, the mean metallicity correction of $\mu^0(\text{Gal})$ of the ten calibrating galaxies amounts to only $\Delta\mu_Z = 0.022$. It is therefore likely that the metallicity corrections affect the zero-point of the distance scale by ≤ 0.10 mag.

That this estimate is realistic is further supported by the comparison in Paper IV of the metallicity-corrected moduli μ_Z^0 with independent TRGB and velocity distances, by the (near) independence of the luminosity of the calibrating SNeIa on metallicity, and by the fact that the metal-rich and metal-poor Cepheids in NGC 5457 (M101), as published by Kennicutt et al. (1998), yield the same distance with the present metallicity corrections.

One proviso is added. In Paper IV it was explained that an average subsolar abundance was adopted for the Galactic Cepheids ($\langle[\text{O}/\text{H}]\rangle = 8.60$). A solar abundance of 8.70 is not completely excluded because the O lines are weak (Kovtyukh et al. 2005). In that case the slope of the metallicity corrections would become shallower and the distances of the 10 parent galaxies of the calibrating SNeIa would decrease by 0.037 mag on average.

b. The adopted zero-point of the distance scale is a source of systematic error. Actually the present distance scale depends on two zero-points, one for the Galactic and one for the LMC P - L relation. The Galactic P - L relation was calibrated in Paper II in equal parts by 33 Cepheids in open clusters and by BBW distances of 36 Cepheids. The clusters are fitted to the ZAMS of the Pleiades at $\mu^0 = 5.61$ mag; this well determined value rests on several determinations including the *trigonometric* HIPPARCOS parallax (Makarov 2002). It was discussed in Paper IV that the calibrating clusters have solar metallicity on average, thus the ZAMS fitting is justified. The BBW luminosities taken from Fouqué et al. (2003) and Barnes et al. (2003) are fainter at $\log P = 1.5$ than those from clusters by 0.11, 0.14, and 0.21 mag in B , V , and I . They may indeed be somewhat faint for arguments discussed in Paper II. They are also fainter by 0.24 ± 0.08 mag than the seven Cepheids with interferometric diameter measurements (Kervella et al. 2004). But averaging in these additional determinations with their proper weights moves the adopted Galactic zero-point by less than 0.10 mag.

The LMC zero-point rests on an adopted weighted modulus of $(m - M)_{\text{LMC}}^0 = 18.54$ as derived in Paper I from 13 determinations by various authors, yet excluding distances

based on the P - L relation of Cepheids. Eclipsing binaries give usually rather lower distances (e.g. Fitzpatrick et al. 2003), but the particularly well determined distance of HV982 of 18.50 ± 0.05 (Fitzpatrick et al. 2002) is compatible with the adopted modulus. It is also in good agreement with more recent determinations, i.e. 18.59 ± 0.09 from the TRGB (Sakai et al. 2004), 18.52 ± 0.03 from K magnitudes of RR Lyr stars based on Bono’s et al. (2003) semi-theoretical zero-point (Dall’Ora et al. 2004), 18.53 ± 0.06 from the BBW method (Gieren et al. 2005) and $18.55 (\pm 0.10)$ from RR Lyr stars (Sandage & Tammann 2006a). It is therefore unlikely that the LMC zero-point is off by as much as 0.10 mag.

The distances of the ten galaxies calibrating the SNIa luminosity are secured by the Galactic *and* LMC zero-points. The error of their combined weight must be smaller than 0.10 mag.

c. In Paper IV (§ 6 there) it was pointed out that Cepheid distances are always dependent on period if the observed slopes in V and I are not identical to the corresponding slopes of the P - L relations used for calibration. The dependence of the adopted distances μ_Z^0 on period was expressed by a π -factor such that $\Delta\mu_Z^0 = \pi \cdot \Delta \log P$. The Cepheids of the ten calibrating galaxies have an overall mean period of $\langle \log P \rangle = 1.45$ (28 days) and $\langle \pi \rangle = 0.40 \pm 0.32$ (Table A1 in Paper IV). If future discoveries of fainter Cepheids will decrease the mean period to say 20 days ($\langle \log P \rangle = 1.30$) the galaxy distances will decrease by 0.06 mag on average. This estimate is an oversimplification because it is foreseeable that additional Cepheids will change the observed slope of the P - L relations and hence also the value of π , but it serves to illustrate the uncertainty inherent in Cepheid distances.

Adding the various error sources in quadrature gives a total systematic error of 0.17 mag. The corresponding error on H_0 is $\Delta H_0 = 5.0$.

4.4. Previous Determinations of H_0 with SNe Ia as Standard Candles

Over the past 24 years a number of attempts have been made to use SNe Ia as standard candles and to derive – after their luminosity has been calibrated in a few nearby cases – the large-scale (or not so large-scale) value of H_0 . Table 6 lists 24 original papers which are devoted to this aim.

It is amusing to note that the overall mean of the 24 determinations of H_0 in Table 6 is 63.5 ± 1.5 , i.e. very close to the present result. However, the seeming agreement is fortuitous, because the individual determinations are based on different P - L relations, different calibrators, different absorption corrections, and on different metallicity and decline rate corrections, if any such corrections are applied at all. The wide variation of H_0 in Table 6 is

therefore mainly due to systematic effects. It is, however, noteworthy that over the last 20 years all values of H_0 agree within their quoted errors with only three or four exceptions.

The values of our team (Saha et al. 1994-2001; Parodi et al. 2000; present paper) have increased over the years from 52 to 62. The lowest value had still to rely on a uncertain calibration through the brightest stars in only two parent galaxies, and one of the calibrators, SN 1954a, turned later out to belong to the overluminous class of which SN 1991T is the prototype. Also SN 1895B, which was used in the first papers, may belong to this class because it is 0.25 mag brighter than SN 1972E in the same galaxy (NGC 5253). Two other eventually discovered effects went also into the direction of increasing H_0 . The decline rate correction, first quantified by Phillips (1993), increases (in its present form) H_0 by 3 units, and the passage from a $\Omega_M = 1$ universe to $\Omega_M = 0.3$, $\Omega_\Lambda = 0.7$ brought an additional increase of 0.8 units.

The latest increase of H_0 by 6.5% over our value in Saha et al. (2001) is due to an accumulation of small effects. It should first be noted that the values M_{BVI} and C_{BVI} here are reduced to $\Delta m_{15} = 1.1$ and $(B-V)^{\text{corr}} = -0.024$, while the reference values were $\Delta m_{15} = 1.2$ and $(B-V)^{\text{corr}} = -0.01$ in 2001. This affects *equally* the apparent magnitudes m_{BVI}^{corr} of the calibrators and the intercepts C_{BVI} of the distant SNe Ia, and has no effect on H_0 . However, the reduction of the absorption factor \mathcal{R}_{BVI} for the dust absorption of SNe Ia in the host galaxy of originally 4.3, 3.3, and 2.0 to the present values 3.65, 2.65, and 1.35 makes the more highly reddened calibrators (see Table 5) fainter by 0.03 mag relative to the distant SNe Ia, which now increases H_0 by 1.5%. Also the coefficients a_{BVI} of the Δm_{15} correction had to be increased for reasons explained in Paper III; this dims the calibrators with their higher $\langle \Delta m_{15} \rangle$ (see Table 5) more than the distant SNe Ia by 0.02 mag on average (1%). A further increase comes from the new photometry of SN 1998aq (1%) and the arrival of the slightly faint tenth calibrator, SN 1998ae, (0.6%). Finally the adopted Cepheid distances μ_Z^0 of the calibrating host galaxies, as derived in Paper IV from new $P-L$ relations and new metallicity corrections and used in Table 1, are 1% smaller than those in Saha et al. (2001), the latter containing a bulk metallicity correction of 0.06 mag and resting on a slightly brighter zero-point of $(m - M)_{\text{LMC}}^0 = 18.56$. These effects together increase our 2001-value of 58.7 ± 2.0 to 61.7 ± 2.1 , which is statistically the same as the present value of 62.3 ± 1.3 .

4.4.1. Comparison of H_0 with Freedman et al. (2001)

One of the strongly deviating H_0 values in Table 6 is from Freedman et al. (2001), whose value of $H_0 = 72$ has been widely adopted. These authors have derived the Cepheid distances

of the host galaxies of their six calibrating SNeIa from the single-fit LMC P - L relations of Udalski et al. (1999), a zero-point of $(m - M)_{\text{LMC}}^0 = 18.50$, and including a metallicity correction close to Kennicutt et al. (1998). These P - L relations are now untenable (Paper II). If one applies the P - L relations of LMC of Paper II, with their break at $P = 10$ days, to the same six SNIa-calibrating galaxies their moduli increase by 0.17 mag, or – after application of the same metallicity correction – by even 0.23 mag. Further, with the adopted moduli μ_Z^0 from Table 1, column (12), which contain the period-dependent metallicity correction of Paper IV, the discrepancy increases to 0.35 mag. With our moduli Freedman et al. (2001) would have obtained $H_0 = 60.4$. Thus their very high value of H_0 is solely caused by their (too) small distances compared with ours. In particular it is *not* due to differences of the HST-based Cepheid magnitudes, because the Freedman team have reproduced them in seven of our program galaxies to within a few 0.01 mag (Gibson et al. 2000, Table 3). – The almost equally high value of H_0 by Altavilla et al. (2004) is based on eight calibrators of Saha et al. (2001) plus the overluminous SN 1991T, but their result is not independent of Freedman et al. (2001) because they have adopted the Cepheid distances of the latter source. In addition they have applied two versions of a theoretical metallicity correction which changes sign about at the metallicity of Galactic Cepheids, independent of period. Their final moduli are smaller than ours on average by 0.33 to 0.43 mag. Using our moduli, they would have obtained $H_0 = 58$ – 61 . It is no surprise that Wang et al. (2006) found for H_0 the same value as Freedman et al. (2001) because they used for their calibrators the Cepheid distances of the latter source.

4.4.2. Comparison of H_0 with Riess et al. (2005)

The most deviating value of H_0 in Table 6 comes from Riess et al. (2005). It is based on only four calibrators whose Cepheid distances were derived from the LMC P - L relations of Thim et al. (2003), which are a slightly earlier version of those in Paper II, but with $(m - M)^0 = 18.50$ and including a metallicity correction from Sakai et al. (2004). The mean metallicity of the four calibrators is very close to the Galactic value. Hence it would have been a more obvious choice to use the *Galactic* P - L relation of Paper II. In that case the authors would have found $H_0 = 63.1$ instead of $H_0 = 73$. This is close to the value 63.3 ± 1.9 from the present metallicity corrected moduli μ_Z^0 of the four calibrators. Riess et al. (2005) have excluded six calibrators as being too old or too heavily absorbed, yet we find for these six SNeIa $H_0 = 61.0 \pm 2.0$, which is the same within statistics as for their four calibrators. Clearly, the authors’ result is not due to the choice or treatment of their calibrating SNeIa, *but only to the fact that they apply a P - L relation for metal-poor Cepheids to a sample of metal-rich Cepheids*. Their correction for metallicity is insufficient, particularly because

their calibrating Cepheids have exceptionally long periods ($\langle P \rangle = 35$ days) and require large corrections.

5. THE LOCAL VALUE OF H_0

The global value of H_0 in § 4 considered only SNe Ia in the velocity range $3000 < v < 20\,000$ (or $30\,000$) km s^{-1} . It remains the interesting question as to the mean “local” value of H_0 , say within 2000 km s^{-1} . This question is pursued in the following sections using Cepheid distances, local SNe Ia, the mean cluster distances of Virgo and Fornax, as well as 21cm-line width and TRGB distances.

Since small distances, down to ~ 2 Mpc, and small velocities are considered here, care is taken to correct them appropriately. All distances in this paragraph refer to the barycenter of the Local Group, assumed at $2/3$ (0.54 Mpc) of the distance towards M 31 (Sandage 1986); these distances are denoted with r_0 or μ_0^0 .

The heliocentric velocities v_\odot of the galaxies are corrected for the solar motion with respect to the barycenter of the Local Group following Yahil et al. (1977). Similar solar-motion solutions by Sandage (1986) and Richter et al. (1987) lead to slightly larger scatter of the Hubble diagram of nearby galaxies. The more deviating solution by Karachentsev & Makarov (2001) causes still larger Hubble scatter; the solution may be influenced by orbital velocities of companion galaxies moving about a larger galaxy. The solar-motion-corrected velocities v_0 are then reduced to v_{00} , which are the velocities as seen from the barycenter of the Local Group. This (small) correction is only viable on the assumption that the observed recession velocities are strictly radially away from the barycenter. Finally the velocities v_{00} are corrected for a self-consistent Virgo-centric infall model with a local infall vector of $\vec{v} = 220 \text{ km s}^{-1}$ and an adopted R^{-2} density profile of the Virgo complex (Yahil et al. 1980; Tammann & Sandage 1985; Kraan-Korteweg 1986), where $v_{220} = v_{00} + \Delta v_{220}$. These authors have calculated Δv_{220} without knowledge of the galaxy distances from v_0 , \vec{v} , and the mean velocity of the Virgo cluster $\langle v_0 \rangle$. In the present case, where all galaxy distances are known, it is easier to use

$$\Delta v_{220} = 220 \left(\cos \alpha + \frac{r_0(\text{Virgo})}{R(\text{galaxy})} \cdot \cos \beta \right) \text{ km s}^{-1}, \quad (5)$$

where $r_0(\text{Virgo})$ is the distance of the Virgo cluster, $R(\text{galaxy})$ is the distance of the galaxy from M 87, α is the angle of the galaxy away from M 87 as seen from the barycenter, and β is the angle of the barycenter away from M 87 as seen from the galaxy. The route through equation (5) is here actually preferable because the errors of the small distances r_0 are small compared to the errors of v_0 , which may be contaminated by important peculiar velocities.

5.1. $H_0(\text{local})$ from Cepheids

The velocity field within 2000 km s^{-1} is mapped in Figure 4 by 25 galaxies, including four members of the Virgo cluster and three members of the Fornax cluster, whose Cepheid distances are taken from Paper IV (Table A1). The cluster members are plotted with the mean cluster velocity. Also shown as open symbols are four galaxies with $\mu_{Z0}^0 < 28.2$ and six galaxies, which are not members of the Virgo cluster, but with angular distances from the cluster smaller than $\alpha_{M87} < 25^\circ$. The four nearby galaxies are not used for the solution because the contribution of their peculiar velocities may be important. The six field galaxies with $\alpha_{M87} < 25^\circ$ will be discussed below.

The distances μ_{Z0}^0 and velocities v_{00} , all reduced to the Local Group barycenter, of the 25 galaxies give a small Hubble constant (57.2 ± 2.5) and large scatter ($\sigma_m = 0.46 \text{ mag}$), (Fig. 4a). If, however, the velocities are corrected for Virgocentric infall the scatter is significantly reduced to $\sigma_m = 0.32 \text{ mag}$ and $H_0(\text{local})$ becomes 62.3 ± 1.9 (Fig. 4b).

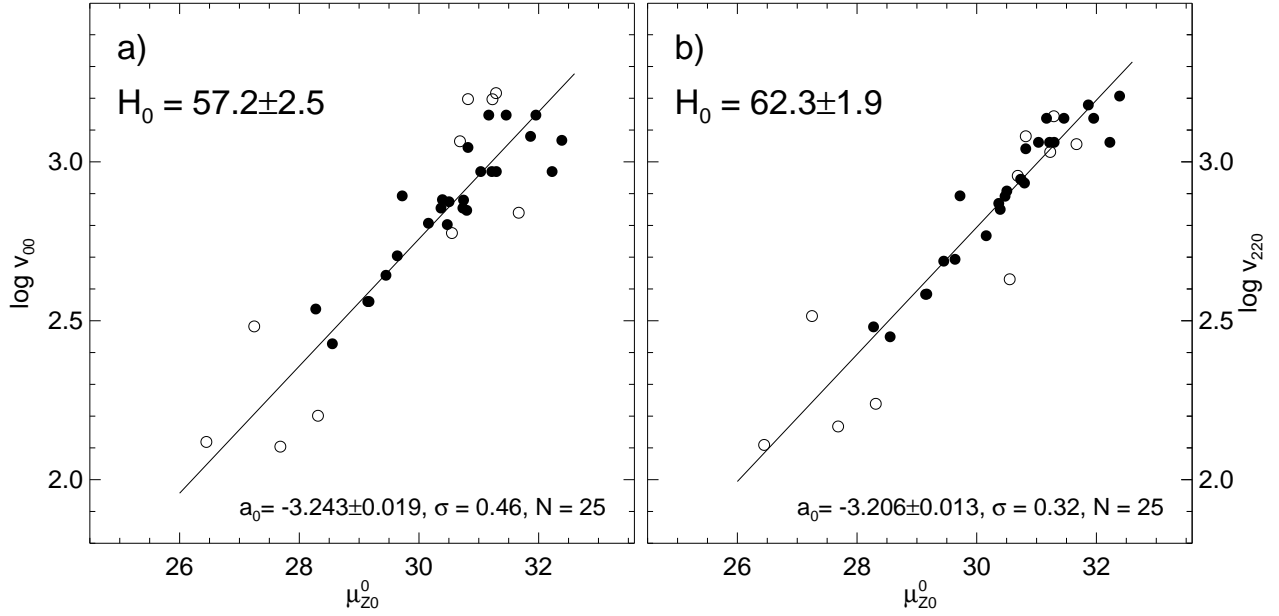


Fig. 4.— The distance-calibrated Hubble diagram using 18 galaxies and 7 Virgo or Fornax cluster members with Cepheid distances (filled symbols). Galaxies within 25° from the Virgo cluster (M87), but outside the cluster, and with $\mu_{Z0}^0 < 28.2$ are shown as open symbols. a) using velocities v_{00} reduced to the gravicenter of the Local Group. b) using velocities v_{220} corrected in addition for Virgocentric infall. The fitted Hubble lines $\log v = 0.2\mu + a_0$ are only through the filled symbols.

5.2. H_0 (local) from nearby SNe Ia

Fully corrected apparent V magnitudes at maximum are given in Paper III for 16 SNe Ia with $v_0 < 2000 \text{ km s}^{-1}$. Their magnitudes are combined with the weighted absolute magnitude of $M_V = -19.46$ from Table 3 to obtain distance moduli μ^0 , which are transformed, as before, to distances μ_0^0 from the Local Group barycenter. The latter are plotted in a Hubble diagram in Figure 5 (filled symbols). The velocities v_{00} , again corrected to the barycenter, give large scatter ($\sigma_m = 0.54 \text{ mag}$) and a small value of $H_0 = 54.3 \pm 3.5$ (Fig. 5a), but after a correction for Virgocentric infall these numbers become $\sigma_m = 0.39 \text{ mag}$ and $H_0 = 58.9 \pm 2.7$ (Fig. 5b), i.e. the value of H_0 is statistically the same as on large scales (equation 4).

One nearby SN Ia with $\mu_0^0 < 28.2$ and six SNe Ia within the 25° ring about the Virgo cluster have not been used for the solution for the same reason given in § 5.1. They are shown as open symbols in Figure 5.

The data of the Cepheids in Figure 4 and of the local SNe Ia in Figure 5 are combined in the Hubble diagram of Figure 6, where only v_{220} velocities are shown. The 28 high-weight distances of field galaxies are plotted, as before, as filled symbols. They define a Hubble line corresponding to $H_0 = 60.4 \pm 1.7$ and $\sigma_m = 0.33 \text{ mag}$ (Fig. 6a). This result is only slightly changed by adding the 13 Virgo and Fornax cluster members from § 5.3 to become

$$H_0 = 60.9 \pm 1.3, \quad \sigma_m = 0.28 \text{ mag}, \quad (6)$$

which we adopt for the local value. We emphasize again the agreement with the global value.

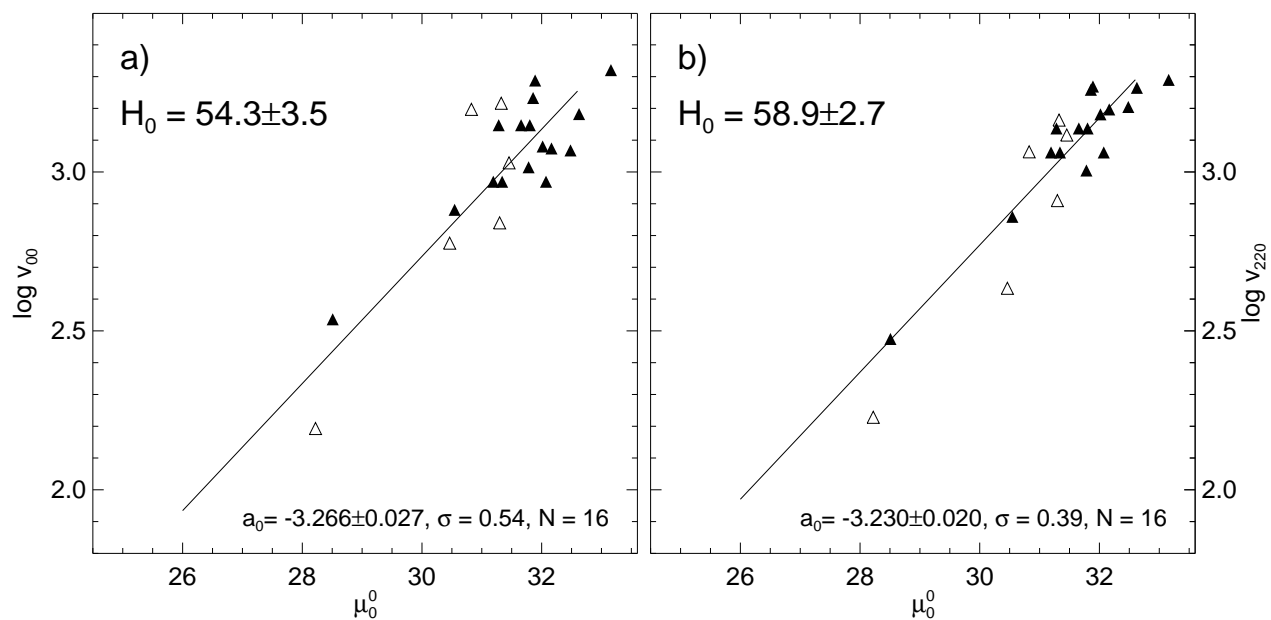


Fig. 5.— The distance-calibrated Hubble diagram of SNe Ia with $v_{220} < 2000 \text{ km s}^{-1}$. Those outside the Virgo cluster but within 25° from the cluster center (M87) and those with $\mu_0^0 < 28.2$ are shown as open symbols. a) using velocities v_{00} reduced to the gravicenter of the Local Group. b) using velocities v_{220} corrected for Virgo-centric infall. The fitted Hubble lines are only through the filled symbols.

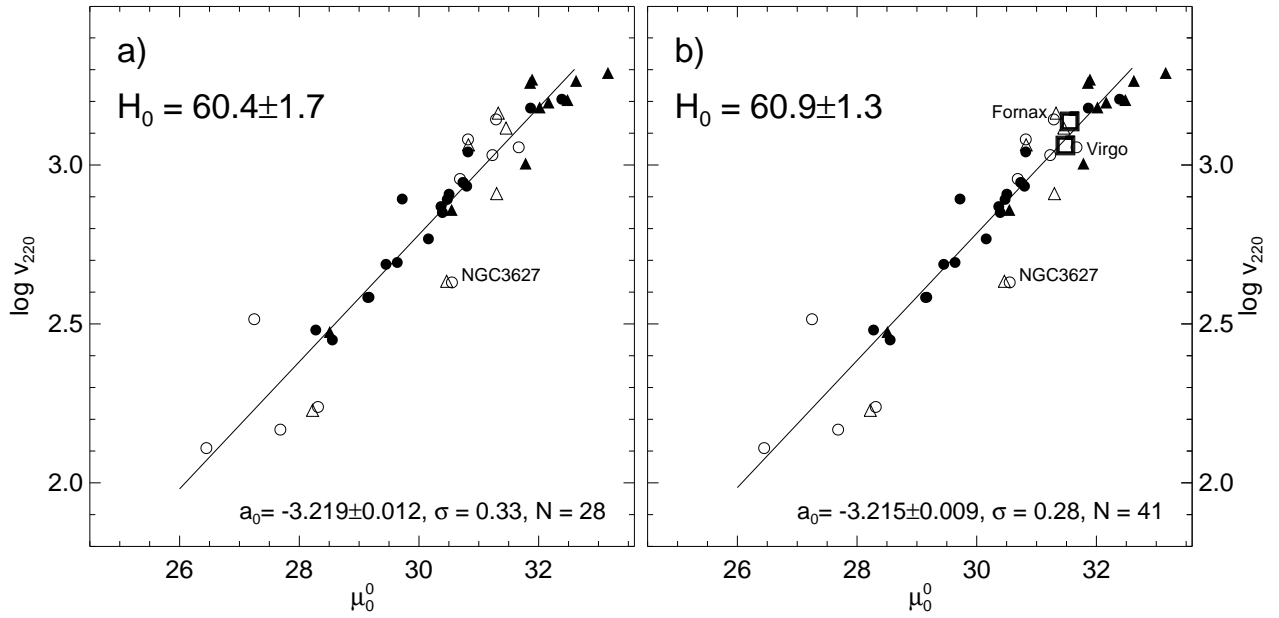


Fig. 6.— The combined distance-calibrated Hubble diagram of field galaxies with Cepheid distances (circles) and of SNe Ia (triangles). Objects inside 25° from the Virgo cluster (M 87) and those with $(m - M)^0 < 28.2$ are shown as open symbols. The Hubble line is fitted to only the filled symbols. b) the Virgo and Fornax clusters are added at their mean distance and mean velocity (from Table 7).

Objects with $\mu_0^0 < 28.2$ are shown as open symbols in Figure 6. They are not used for equation (6), although their inclusion would not change H_0 , but it would increase the scatter (due to the *relatively* large peculiar motions).

The 15 galaxies with distances from Cepheids or SNe Ia, which are shown as open symbols in the upper part of Figure 6, lie in a ring of radius 25° about the Virgo cluster. Their separate treatment here is a precaution because it may be suspected that the surroundings of a cluster have particularly large peculiar velocities. This seems supported by a Hubble diagram plotting $\log v_{00}$ versus μ_0^0 , where the scatter is as high as $\sigma_m = 0.72$ mag. Even if the deviating galaxy NGC 3627 is excluded, the scatter remains high at $\sigma_m = 0.45$ mag. However, if the velocities are corrected for Virgocentric infall the scatter reduces to $\sigma_m = 0.31$ which is even less than $\sigma_m = 0.33$ from the field galaxies outside the 25° ring. Two conclusions follow: (1) the region about the Virgo cluster is hardly more turbulent than the general field, and (2) the Virgocentric infall model, which already efficiently reduced the velocity scatter in Figure 4 and 5, is surprisingly successful even in regions close to the cluster.

The agreement of $H_0(\text{local}) = 60.9 \pm 1.3$ and $H_0(\text{global}) = 62.3 \pm 1.3$ does not mean that the Hubble flow is unaltered by gravity, because it must be stressed again that a selfconsistent Virgocentric infall model with a local infall vector of 220 km s^{-1} has been subtracted from the observed velocities to compensate for the excess gravity of the cluster.

An interesting by-product of Figure 6a is its small scatter of $\sigma_\mu = 0.33$ mag, which is reduced to 0.28 mag if an average error of 0.15 mag of the distance determinations is allowed for. This implies that peculiar motions contribute to the scatter with only $\partial v/v = 0.14$, and hence that in the distance interval of $500 \lesssim v \leq 1500 \text{ km s}^{-1}$ the peculiar velocities of field galaxies are restricted to $70 - 210 \text{ km s}^{-1}$.

5.3. $H_0(\text{local})$ from the Distance of the Virgo and Fornax Clusters

Cepheid and SNe Ia distances of Virgo and Fornax cluster members render themselves for a distance determination of the two clusters. The relevant data are shown in Table 7, where the Cepheid distance moduli are taken from Paper IV (Table A1, col. [9]). The SN Ia moduli are the difference between the fully corrected apparent magnitudes m_V from Paper III (Table 2, col. [9]) and the absolute magnitude $M_V = -19.46$ (from Table 3, col. [12]). The 21cm-line width distance of the Virgo cluster is from below (§ 5.4).

In the case of the Virgo cluster the two SNe Ia 1960F (NGC 4496A) and 1981B (NGC 4536) are omitted, because they do not lie in the cluster proper, but in the complex W-cloud (Binggeli et al. 1993). Also SN 1999cl (NGC 4501) is omitted because of its large absorption

(Paper III). However, SN 1990N (NGC 4639) is included in Table 7 as a bona fide member of the Virgo cluster in spite of its large distance. Its recession velocity agrees almost exactly with the cluster mean. The galaxy has gravitationally interacted with NGC 4654, which shows additional effects of ram pressure from the cluster X-ray gas (Vollmer 2003). Moreover, if NGC 4639 was a field galaxy in the cluster background its distance and $H_0 = 62$ would require a recession velocity higher than observed by $\sim 500 \text{ km s}^{-1}$. A peculiar velocity of this size of NGC 4639 and NGC 4654 would be very unusual for field galaxies.

While NGC 4639 clearly lies on the far side of the Virgo cluster, the three remaining Virgo galaxies with Cepheid distances (NGC 4321, 4535, and 4548) are on the near side, because they have been selected for the HST observations on the basis of their above average resolution (Sandage & Bedke 1988). The effect of this bias has been neglected by Freedman et al. (2001) and others. High resolution galaxies do indeed favor an incorrect small mean distance of the Virgo cluster if used alone (Tammann et al. 2002, Fig. 7). The difficulty to determine the exact Virgo cluster distance lies in the fact that its extent in depth ($\sim 10 \text{ Mpc}$) is significantly larger than its projected radius.

Table 7 lists also a Virgo cluster distance from the 21cm-line width method (see § 5.4 below). The cluster distance modulus of 31.65 ± 0.08 ($\sigma_\mu = 0.59$) is derived from a *complete* sample of 49 inclined Virgo cluster spirals, as compiled by Federspiel et al. (1998), and from the Cepheid-based calibration of the method in equation (8) below. The distance, however, has been reduced by 0.07 mag for the fact that the cluster members at a given line width are redder in $(B-I)$ on average and also HI-deficient if compared with the calibrating field galaxies (see Federspiel et al. 1998, § 8). As a consequence our adopted TF distance of the Virgo cluster becomes $\mu_0 = 31.58 \pm 0.08$. [See also Sandage & Tammann (2006b) for a less restricted sample of Virgo cluster galaxies giving $\mu_0 = 31.60 \pm 0.09$].

The unweighted distances of the Virgo and Fornax cluster are shown in Table 7 as well as their velocities. The adopted velocity of the Virgo cluster of 1165 km s^{-1} is the mean of v_{220} and the *independent* value of v_{cosmic} from Jerjen & Tammann (1993). The ensuing values of H_0 are 58.1 ± 4.6 from Virgo and 66.8 ± 4.0 from Fornax. To emphasize, our distances to the Virgo and Fornax cluster are $\sim 0.7 \text{ mag}$ more remote than derived by Freedman et al. (2001), signalling the $\sim 14\%$ difference in our respective values of H_0 .

5.4. H_0 (local) from 21cm-Line Widths

Several global properties of galaxies correlate with the galaxian luminosity or diameter, e.g. the morphological luminosity classes of van den Bergh (e.g. van den Bergh 1960a,b;

Sandage 1999), 21cm-line widths (TF; e.g. Tully & Fisher 1977; Sakai et al. 2000) of spirals or the surface brightness fluctuations (SBF; e.g. Tonry & Schneider 1988; Tonry et al. 2000) and velocity dispersion-diameter relation ($D_n - \sigma$ or “fundamental plane”; e.g. Faber & Jackson 1976; Dressler et al. 1987; Djorgovski & Davis 1987; Kelson et al. 2000) of early type galaxies. Their zero-point calibration depends directly or indirectly on Cepheids, and they are therefore sensitive to any change of the distance scale of Cepheids. The disadvantage of these methods is their large intrinsic scatter ($\sigma_M > 0.3$ mag), which makes them, if applied to *apparent-magnitude-limited* (and often even to incomplete distance-limited) galaxy samples, susceptible to observational selection bias (of which Malmquist is an example), *leading always to too high values of H_0* . For large samples, methods have been devised to compensate for such biases in first approximation (Bottinelli et al. 1988; Federspiel et al. 1994; Sandage 1994, 1996; Teerikorpi 1987, 1990, 1997).

One of the few examples of an (almost) *complete distance-limited* sample, which is immune to observational selection bias, has been compiled by Federspiel (1999) for spirals with inclination $i > 45^\circ$ and $v_0 \leq 1000 \text{ km s}^{-1}$. The apparent magnitudes B_T of the 114 sample galaxies are taken from the RC3 (de Vaucouleurs et al. 1991) or, if not available, the apparent magnitudes m_B are used as listed in the NASA/IPAC Extragalactic Database (NED, <http://nedwww.ipac.caltech.edu>). Most of the 43 m_B 's come originally also from the RC3 and are in the same system as the B_T 's. The magnitudes are corrected for Galactic absorption following Schlegel et al. (1998) and for the inclination dependent total internal absorption, which are determined as described in the Introduction to the RSA. The necessary galaxian axis ratios a/b are taken from the RC3. The line widths w_{20} are taken from the same source where available. In 15 cases they are the mean of all $\log w_{20}$ values given in the Lyon Database for physics of galaxies (HyperLeda, <http://leda.univ-lyon1.fr>). Many galaxies with line widths in both catalogs reveal a systematic inclination-dependant difference of

$$\Delta \log w_{20} = -0.003i + 0.203 \tag{7}$$

in the sense of RC3 – HyperLeda. The additional line widths have been reduced to the system of the RC3 by means of equation (7).

There are 31 galaxies with known apparent magnitudes B_T and line widths w_{20} from the RC3 for which Cepheid distances are available from Paper IV (Table A1). After correction for Galactic and internal absorption and in the case of w_{20} for inclination they define the calibration of the TF relation (Fig. 7):

$$M_B = -7.31 \log w_{20} - (1.822 \pm 0.090), \sigma = 0.51. \tag{8}$$

The slope of -7.31 was determined from Virgo cluster members by Federspiel et al. (1998) making allowance for errors of the apparent magnitudes and of $\log w_{20}$ and for the depth

effect of the cluster. However, the slope is not well determined. Changing the assumptions on the errors, or determining the slope from the Cepheid-calibrated galaxies (in spite of their restricted range in $\log w_{20}$) can change the slope by a full unit in either direction. Fortunately this affects the *mean* cluster distance by only a few 0.01 mag. The 31 calibrators give a scatter of the TF relation of $\sigma_{MB} = 0.51 (\pm 0.09)$ mag, which is (insignificantly) larger than $\sigma_{MB} = 0.43 (\pm 0.10)$ mag found by Sakai et al. (2000) from 21 calibrators. If equation (8) is applied to the 111 galaxies in the 1000 km s^{-1} sample one obtains their distances, which are plotted with their corresponding recession velocities ($\log v_{220}$) in Figure 8. Excluding galaxies with $v_{220} < 200 \text{ km s}^{-1}$ and three strongly deviating galaxies, one obtains an intercept of the Hubble line of $a_0 = -3.229 \pm 0.014$, which corresponds to $H_0 = 59.0 \pm 1.9$. The solution is remarkably robust. The galaxies with $\log w_{20} \leq 2.4$ yield $H_0 = 59.3$ and 58.2 , respectively. The 16 field galaxies inside the 25° about the Virgo cluster yield, again in statistical agreement, $H_0 = 60.6$ (cf. § 5.2). The scatter of $\sigma_\mu = 0.69$ mag in Figure 8 (or $\sigma_\mu = 0.63$ mag for $\log w_{20} > 2.4$) is surprisingly large, i.e. even larger than for the spirals in the Virgo cluster ($\sigma_m = 0.59$ mag) in spite of its depth effect. Yet, if allowance is made for a scatter of ~ 0.3 due to peculiar motions, the TF scatter in B is reduced to $\sigma_\mu = 0.62$ mag (or 0.55 mag for fast rotators). The still rather large scatter is not due to the mixture of B_T and m_B magnitudes because the scatter of the latter is only insignificantly larger. Errors of other observational parameters (inclination, internal absorption, line width) particularly of the fainter sample members may blow up the scatter, but just the faintest galaxies are essential for a complete distance-limited sample. This illustrates the high price paid in using samples with large σ_M due to the always present observational selection biases. In principle it would advantageous to use I magnitudes for the TF method, because the corrections for internal absorption are smaller here but the paucity of available standard I magnitudes prevents the definition of complete, *distance-limited* samples.

Notwithstanding these difficulties, the mean value within 1000 km s^{-1} of $H_0 = 59.0 \pm 1.9$ from the TF relation for 104 field galaxies agrees with the evidence from the smaller Cepheid and SN Ia samples. Of course, this statement must be relativated because the results are not independent since the TF relation has been calibrated using the Cepheid distances.

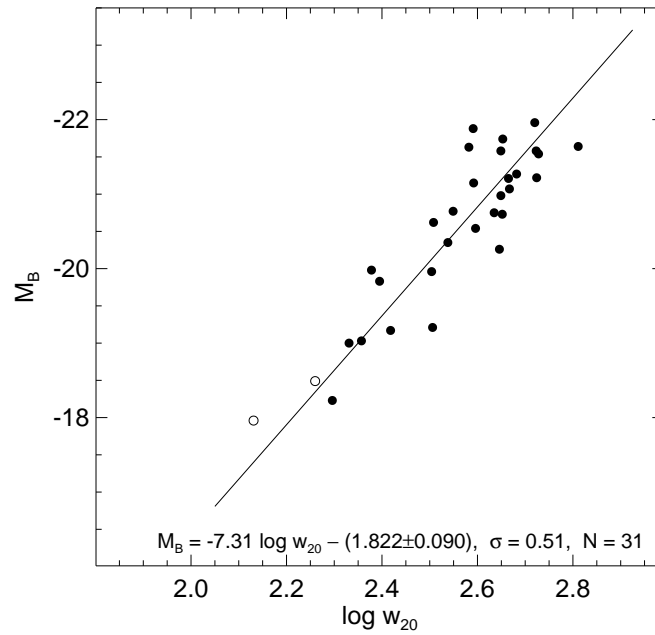


Fig. 7.— The calibration of the 21cm-line width – absolute magnitude relation by means of 31 inclined galaxies with known Cepheid distances. The companion galaxies NGC 5204 and 5585, shown as open symbols, are assumed at the same distance as M 101. The scatter is much larger than can be accounted for by the error of the Cepheid distances.

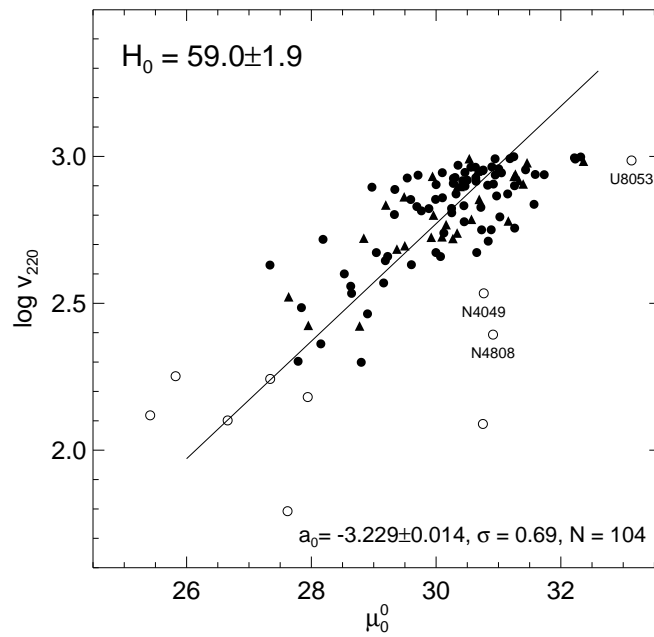


Fig. 8.— The distance-calibrated Hubble diagram of a complete sample of 114 inclined spirals with Tully-Fisher distances and with $v_{220} < 1000 \text{ km s}^{-1}$. Galaxies with $\log w_{20} \geq 2.4$ are shown as triangles, galaxies with $\log w_{20} < 2.4$ as dots. Galaxies with $v_{220} < 200 \text{ km s}^{-1}$ and three deviating galaxies are shown as open symbols; they are not used for the solution. Note the large scatter. Member galaxies of the Virgo cluster are not shown.

5.5. $H_0(\text{local})$ from TRGB Distances

TRGB distances are of fundamental importance because they rest entirely on Pop. II stars and are hence *independent of any Cepheid distances*. The brightness of the TRGB is based on globular clusters (Da Costa & Armandroff 1990; Lee et al. 1993; Bellazzini et al. 2001); its I -magnitude is, according to theoretical models (Cassisi & Salaris 1997; Sakai et al. 2004), only moderately dependent on metallicity. The disadvantage of the method is that its range is restricted, even with HST, to ~ 10 Mpc.

In Paper IV the TRGB distances of nine galaxies by Sakai et al. (2004), for which also Cepheid distances are available, were already used to confirm the zero-point of the Cepheid distance scale to within ~ 0.1 mag and to demonstrate that the adopted Cepheid distances carry no noticeable metallicity effect.

Here many additional TRGB distances are used to determine a very local value of H_0 and to compare it with the *independent* evidence from § 5.1 – 5.4.

Karachentsev et al. (2004, 2005) have determined TRGB distances with HST for well over 100 galaxies of all types, including many dwarf galaxies. Excluding as before galaxies with $\mu_0^0 < 28.2$ leaves 43 galaxies, to which we have added five galaxies from Sakai et al. (2004). While Karachentsev et al. have adopted a uniform zero-point of the TRGB of $M_B = -4.05$ mag, Sakai et al. have applied small corrections for metallicity, but their mean zero-point of -4.01 mag is sufficiently close not to make a difference in the following. One may wonder whether the zero-point of the TRGB method is indeed stable over a magnitude range of the galaxies from -10 to -20 mag, i.e. a factor of 10^4 in luminosity. Tests show that $\langle H_0 \rangle$ varies by merely $\sim \pm 3\%$ if only the faintest or only the brightest galaxies (giving a lower H_0) are considered. If real, this may be a metallicity or a population size effect, but it is small enough to be neglected here.

The 59 galaxies (excluding the deviating case D634-03) with TRGB distances $\mu_0^0 > 28.2$ are plotted in a distance-calibrated Hubble diagram in Figure 9 (filled symbols). Using v_{00} velocities as seen from the Local Group barycenter yields $H_0 = 57.6 \pm 1.6$, which is increased to the adopted value of $H_0 = 61.7 \pm 1.5$ after correction for Virgocentric infall. The dispersion about the Hubble line of $\sigma_m = 0.39$ mag, which must be caused mainly by peculiar motions, corresponds to $\partial v/v = 0.20$ or $v_{\text{pec}} = 125 \text{ km s}^{-1}$ at 10 Mpc and $v_{\text{pec}} = 55 \text{ km s}^{-1}$ at 4.4 Mpc.

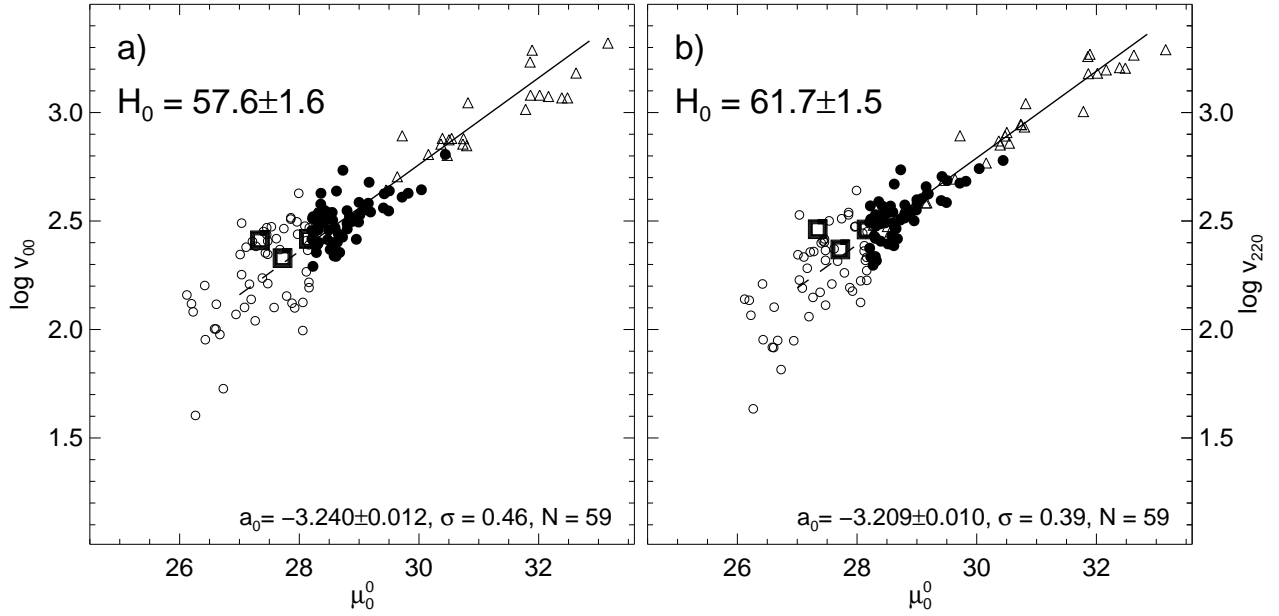


Fig. 9.— The distance-calibrated Hubble diagram of galaxies with TRGB distance moduli (referred to the barycenter of the Local Group) and $\log v_{00}$ (also referred to the barycenter). Open and closed dots are for $\mu_0^0 \leq 28.2$. The adopted SNe Ia and Cepheids of Fig. 6 outside $\alpha_{M87} = 25^\circ$ are shown as open triangles (\triangle) for comparison. The squares stand for the M 81, Cen A, and IC 342 groups. The full line is a fit to the TRGB galaxies with $(m - M)^0 > 28.2$. b) Same as a), but corrected for Virgocentric infall.

It may appear puzzling that Karachentsev (2005) derived $H_0 = 72$ from six very nearby groups with distances from the TRGB and other distance indicators, and $H_0 = 68$ (Karachentsev et al. 2005) from 110 *field* galaxies with distances $2.5 \lesssim r \lesssim 7$ Mpc based on TRGB *and* old Cepheid distances. If, however, we restrict the sample to the 59 field galaxies from above with TRGB distances larger than 4.4 Mpc and proceed along the precepts of Karachentsev et al. (2005), i.e. with distances as seen from the Galaxy (not the barycenter of the Local Group) and velocities reduced to the barycenter following Karachentsev & Makarov (2001), we obtain $H_0 = 58.2 \pm 2.4$, which must be compared with $H_0 = 57.6 \pm 1.6$ from above. We can therefore not reproduce values of $H_0 = 72$ or 68 using *only* TRGB distances.

In the very nearby distance range of $27.0 < \mu_0^0 < 28.2$, i.e. between 2.5 and 4.4 Mpc, are 89 galaxies with TRGB distances from Karachentsev et al. (2004, 2005). Of these 45 galaxies are assigned to the M 81, Cen A, and IC 342 groups as unquestionable members by Karachentsev (2005). Relevant mean parameters of the three groups are compiled in Table 8 and their position in the Hubble diagram is shown in Figure 9 (squares). Column (2) of Table 8 gives the number of available TRGB distances, whose mean is shown in column (3). The velocity $\langle v_{\odot} \rangle$ in column (5) is the mean over all group members with known velocity. The individual values of the Hubble parameter H_i are in column (9). The distance in km s^{-1} of the mean group velocity $\langle v_{220} \rangle$ from the Hubble line with $H_0 = 60.3$ is in column (10). While the first two groups in Table 8 deviate by less than 30 km s^{-1} from the Hubble line, the IC 342 group has an excess velocity of 113 km s^{-1} , which may support the view that the galaxy was early-on ejected from the Local Group (Byrd et al. 1994).

The remaining 44 field galaxies in the nearest distance interval ($27.0 < \mu_0^0 < 28.2$), shown as open dots in Fig. 9, give $H_0 = 63.8 \pm 3.5$ from v_{00} and $H_0 = 64.0 \pm 3.0$ using v_{220} velocities. The dispersion is reduced in the latter case to $\sigma = 0.67$ mag, which translates into random velocities of 65 km s^{-1} at a median distance of 3.2 Mpc. The data are fully consistent with the conclusion that the underlying Hubble flow is linear down to scales of ~ 2.5 Mpc. At still smaller distances the Hubble line curves downwards as a clear effect of the gravitational pull of the Local Group (Lynden-Bell 1981; Sandage 1986).

Following Byrd et al. (1994) Chernin et al. (2004, 2005) have performed model calculations of a possibly violent formation process of the Local Group whereby (some of) the dwarf galaxies may have been ejected into the nearby field. They are predicted to have Hubble ratios of ~ 90 and small velocity dispersion. At most a handful of dwarfs in Figure 9 (open symbols) match this prediction.

The near agreement to better than 5% between H_0 from local Cepheids and SNe Ia ($H_0 = 60.9 \pm 1.3$) as well as from distant SNe Ia ($H_0 = 62.3 \pm 1.3$) on the one hand and H_0

from the *independent* TRGB ($H_0 = 61.7 \pm 1.5$) on the other hand must be emphasized. It suggests, in fact, that the *combined* systematic error of the Cepheids and of the TRGB is not larger than ~ 0.10 mag. In § 4.3 the systematic error of H_0 has been estimated to be 0.17 mag. This appears now like a generous upper limit.

The constancy of H_0 over scales from ~ 2.5 to 200 Mpc, with significant deviations only in and around bound structures, has been a puzzle for a long time (Sandage et al. 1972; Sandage 1986, 1999). The solution that the vacuum energy may be the dominant effect is further discussed in § 7.

6. PHYSICAL DISTANCE DETERMINATIONS

Most astronomical distance determinations need some known distance as a reference point. In this sense even distances from trigonometric parallaxes require knowledge of the Astronomical Unit. In contrast, there are objects whose distance can be determined from only their physical (or geometrical) properties without reference to any astronomical distance. These are referred here to as “physical” distances.

A typical example are the moving-atmosphere distances of Cepheids (the BBW method) which contribute to the zero-point definition of the Galactic P - L relation. Another example is the water-maser distance of NGC 4258 (Herrnstein et al. 1999) as discussed in Paper IV. As more of them become available they too will contribute to the zero-point definition of the P - L relation of Cepheids. The eclipsing binary distance of M 31 of $(m - M)^0 = 24.44 \pm 0.12$ (Ribas et al. 2005) is in satisfactory agreement with its Cepheid distance of 24.54 in Paper IV.

Of particular interest for the present paper are SN Ia models which predict the luminosity of SNe Ia at maximum. Typical results are $M_B \approx M_V = -19.50$ (Branch 1998 for a review) which agrees spectacularly well with our empirically determined value of $M_V = -19.46$ in § 3.2.

“Expanding-atmosphere parallaxes” (EPM) of SNe II have been determined by several authors. The difficulty here is that the radiation transport in fast moving atmospheres poses enormous problems. Five EPM distances of Schmidt et al. (1994) for the five galaxies for which also Cepheid distances are available (Paper IV, Table A1) show good agreement to 0.09 ± 0.13 (the EPM distances being formally larger), but the larger EPM distances suggest an unrealistic increase of H_0 with distance. Only two of Hamuy’s (2001) SN II distances can be compared with Cepheids; the Cepheid distances are larger by ~ 0.5 mag. A recent progress in the “Spectral-fitting expanding atmosphere method” (SEAM) of the type II SN 1999em (Baron et al. 2004) gives $(m - M)^0 = 30.48 \pm 0.30$, which compares favorably with the

Cepheid distance of its parent galaxy NGC 1637 of $\mu_Z^0 = 30.40$. – A different method has been developed for type IIP SNe by Nadyozhin (2003). It uses the expansion velocity and duration of the plateau phase as well as the tail magnitude to yield for eight SNe IIP a value of $H_0 = 55 \pm 5$. However, the result depends on the assumption that the ^{56}Ni energy equals the expansion energy, which requires further testing.

Much effort has gone into the determination of H_0 from the Sunyaev-Zeldovich (SZ) effect. A typical result is $H_0 = 60 \pm 3$, yet with a systematic error of ± 18 (Carlstrom et al. 2002). Also more recent investigations give similar values and errors (e.g., Udomprasert et al. 2004; Jones et al. 2005).

Gravitationally lensed quasars with two or more images provide distances if the redshift of the lens and of the quasar and the delay time between the images are known. Unfortunately the solution is degenerate as to the distance *and* the mass distribution of the lens. Values of H_0 for different sources and by different authors therefore vary still between $48 < H_0 < 75$ (e.g. Saha & Williams 2003; Koopmans et al. 2003; Kochanek & Schechter 2004; York et al. 2005; Magain 2005). Saha et al. (2006) state that the current data are consistent with H_0 anywhere between 60 and 80 at the 1σ level depending on the mass model of the lens.

The last-mentioned method does not in principle provide the (present) value of H_0 , but H_z at the epoch of the quasar. To obtain H_0 some assumptions on Ω_M and Ω_Λ are necessary. The disadvantage of long look-back times for the determination of H_0 becomes most pronounced in case of the Fourier spectrum of the CMB acoustic waves, where a number of free parameters must simultaneously be solved for. The solution for H_0 depends therefore on the number of free parameters allowed for and on some priors forced on the data as well as on the observations used. A six-parameter solution of the WMAP data with some priors and additional observational constraints has yielded $H_0 = 73 \pm 3$ (Spergel et al. 2003, 2006). This has often been taken as a confirmation of $H_0 = 72 \pm 8$ as obtained from various distance indicators by Freedman et al. (2001), and has led to the opinion that the problem of H_0 has been solved. We disagree. The actual situation has been illustrated by Rebolo et al. (2004) who have used the Very Small Array and WMAP data to derive $H_0 = 66 \pm 7$ allowing for twelve free parameters and no priors. Clearly a strong motive to further reduce the systematic error of H_0 by conventional means comes from the desire to use the Hubble constant itself as a reliable prior for the interpretation of the CMB spectrum.

A value of $H_0 = 62.3$ corresponds in an $\Omega_M = 0.3$, $\Omega_\Lambda = 0.7$ universe to an expansion age of 15.1 Gyr, which may be compared with the age of M 92 of 13.5 Gyr (VandenBerg et al. 2002) and the Th/Eu age of the Galactic halo of ~ 15 Gyr (Pagel 2001). Ultra-metal-poor giants yield radioactive ages between 14.2 ± 3.0 to 15.6 ± 4.0 Gyr (Cowan et al. 1999; Westin et al. 2000; Truran et al. 2001; Sneden et al. 2003). A high-weight determination of the

U/Th age of the Milky Way gives 14.5 ± 2.5 Gyr (Dauphas 2005). All these values must, of course, still to be increased by the gestation time of the chemical elements.

7. CONCLUSIONS

(1) The final result of our HST collaboration, ranging over 15 years, is that

$$H_0(\text{cosmic}) = 62.3 \pm 1.3 \text{ (random)} \pm 5.0 \text{ (systematic)} \quad (9)$$

based on 62 SNeIa with $3000 < v_{\text{CMB}} < 20\,000 \text{ km s}^{-1}$ and on 10 luminosity-calibrated SNeIa. All SNeIa have been corrected for Galactic and internal absorption and are normalized to decline rate Δm_{15} and color (Paper III). The weighted mean luminosities of the 10 calibrators of $M_B = -19.49$, $M_V = -19.46$, and $M_I = -19.22$ (Table 4) are based on metallicity-corrected Cepheid distances (Paper IV) from the new P - L relations of the Galaxy and LMC (Paper I & II).

(2) The local value of H_0 ($300 \lesssim v_{220} < 2000 \text{ km s}^{-1}$) is

$$H_0(\text{local}) = 60.9 \pm 1.3 \text{ (random)} \pm 5.0 \text{ (systematic)} \quad (10)$$

from 25 Cepheid and 16 SNeIa distances, involving a total of 34 different galaxies. Their distances are related to the barycenter of the Local Group and their observed velocities are corrected for a self-consistent Virgo-centric infall model with a local infall vector of 220 km s^{-1} . The local value of H_0 is supported by the mean distances and mean velocities $\langle v_{220} \rangle$ of the Virgo and Fornax cluster (Table 7).

(3) The values of H_0 under 1) and 2) find strong support by TRGB distances which constitute an *independent* Pop. II distance scale. Forty-seven TRGB distances in the range from 4.4 Mpc to 10 Mpc yield $H_0 = 60.3 \pm 1.8$. This may suggest that the systematic error in equations (9) and (10) has been overestimated.

(4) The constancy of H_0 from global cosmic scales down to 4.4 Mpc or even 2.5 Mpc (see also Ekholm et al. 2001) in spite of the inhomogeneous mass distribution requires a special agent. Vacuum energy as the solution has been proposed by several authors (e.g. Baryshev et al. 2001; Chernin 2001; Chernin et al. 2003a,b; Thim et al. 2003; Teerikorpi et al. 2005). No viable alternative to vacuum energy is known at present. The quietness of the Hubble flow lends support for the existence of vacuum energy.

(5) The modulating effect of bound structures and their surroundings on the Hubble flow is seen in the immediate neighborhood of the Local Group and particularly clearly in the successful Virgo-centric flow model (see Fig. 4 and 5).

(6) Random velocities of field galaxies at large distances ($5000 < v_{\text{cmb}} < 20\,000 \text{ km s}^{-1}$) are confined by 20 SNe Ia in E/S0 parent galaxies (and hence with little internal absorption). Their scatter about the Hubble line is $\sigma_I = 0.10 \text{ mag}$ (Paper III) which implies $\partial v/v \leq 0.05$ or 250 km s^{-1} at a distance of 5000 km s^{-1} . This is a strict upper limit because no allowance for the intrinsic and observational scatter of the normalized SN Ia luminosities has been made. At intermediate distances ($300 < v_{220} < 2000 \text{ km s}^{-1}$) the scatter from Cepheids and SNe Ia is 0.33 mag without any allowance for observational errors. Therefore $\partial v/v \leq 0.16$, which corresponds to peculiar velocities of ≤ 160 (80) km s^{-1} at a distance of 1000 (500) km s^{-1} . TRGB distances give $v_{\text{pec}} = 60 \text{ km s}^{-1}$ at a distance of 300 km s^{-1} . In the still closer neighborhood of the Local Group the velocity dispersion is similar, emphasizing again the quietness of the Hubble flow.

(7) The adopted value of $H_0 = 62.3$ rests about equally on two zero-points. (i) The zero-point of the Galactic P - L relation of Cepheids which is determined with equal weights from 33 purely physical moving-atmosphere (BBW) parallaxes and 36 Cepheids in Galactic clusters, which are fitted to the ZAMS of the Pleiades at $(m - M)^0 = 5.61$. And (ii) The zero-point of the LMC P - L relation which is based on an adopted LMC modulus of 18.54 from various determinations, but excluding methods which involve the P - L relation itself.

(8) The adopted metallicity corrections of the Cepheid distances are supported by model calculations by Fiorentino et al. (2002) and Marconi et al. (2005) who show that the instability strip shifts redwards in the $\log L - \log T_e$ plane (at $L = \text{const.}$) as the metallicity increases similar to earlier models by authors cited in § 1, but now also for a wide range of $\Delta Y/\Delta Z$. Moreover, the metallicity corrections are supported by comparing the metallicity-corrected moduli μ_Z^0 with independent TRGB and velocity distances. Additional positive tests are provided by the metal-rich and metal-poor Cepheids in NGC 5457 (M 101) and by the (near) independence of the SN Ia luminosities on the metallicity of their parent galaxies.

(9) Several previous authors, listed in Table 6, have found from SNe Ia values of H_0 in statistical agreement with equation (9). The present determination, however, is based on larger data sets and, as we believe, on more realistic P - L relations of Cepheids. Significantly larger values of H_0 in Table 6 are mainly due to the adopted (small) Cepheids distances by others – and not due to the specific treatment of the data on SNe Ia per se, such as the absorption corrections in the parent galaxies, or the normalizations to decline rate and color. Already Germany et al. (2004) have pointed out the large spread of SNe Ia-based determinations of H_0 in the literature is almost entirely due to systematic errors of the Cepheid distances. Had Freedman et al. (2001), e.g., used our Cepheid distances for their six calibrating SNe Ia and their version of the SN Ia Hubble diagram, they would have found $H_0 = 60.5$ instead of 72.

(10) The value of $H_0(\text{cosmic})$ corresponds in a standard Λ CDM ($\Omega_M = 0.3, \Omega_\Lambda = 0.7$) model to an expansion age of 15.1 Gyr, giving a sufficient time frame for even the oldest Galactic globular clusters and highest radioactive ages.

Allan S. needs to make a statement: “Much of the work in this paper has been done by G.A.T., and, although input has been made by all the signed authors, under normal circumstances Tammann would be the lead author. However, G.A.T. and Abhijit S. have conspired to offer as an 80th year birthday gift to me the first-author-place for which I have acquiesced to emphasize the 43 years of a most enjoyable collaboration with G.A.T. and the almost 20 years with Abhijit on this problem. Ours has been a most unusual, productive, and magic scientific time together, working within the SNeIa HST collaboration.” Allan S.’s collaborators thank him for having guided this project as a PI over most of its duration and for his inspiration and incessant drive. We thank collectively the many individuals at STScI who over time made the original observations with HST possible. We also thank several collaborators, particularly Lukas Labhardt and Frank Thim, who have joined us at different stages of our long endeavor. It is a pleasure to thank Susan Simkin, scientific editor, for her sensitivity in seeing this paper on the continuing highly charged debate over H_0 through the editorial process. We also thank the two referees whom she chose for their neutrality, one anonymous and the other Nicholas Suntzeff for their several suggestions for clarity which we have followed. Abhijit S. thanks for support provided by NASA of the retroactive analysis WFPC2 photometry zero-points through grant HST-AR-09216.01A from the Space Telescope Science Institute, which is operated by the Association of Universities for Research in Astronomy, Inc., under NASA contract NAS 5-26555. Bernd R. thanks the Swiss National Science Foundation for financial support. Allan S. thanks the Carnegie Institution for post-retirement facilities support.

REFERENCES

- Alibert, Y., Baraffe, I., Hauschildt, P., & Allard, F. 1999, *A&A*, 344, 551
- Altavilla, G., et al. 2004, *MNRAS*, 349, 1344
- Andrievsky, S.M., et al. 2002, *A&A*, 381, 32
- Ardeberg, A., & de Groot, M. 1973, *A&A*, 28, 295
- Barbon, R., Capaccioli, M., & Ciatti, F. 1975, *A&A*, 44, 267
- Barbon, R., Ciatti, F., & Rosino, L. 1973, *A&A*, 25, 241
- Barnes, T., Jeffreys, W., Berger, J., Mueller, P., Orr, K., & Rodriguez, R. 2003, *ApJ*, 592, 539
- Baron, E., Nugent, P.E., Branch, D., & Hauschildt, P.H. 2004, *ApJ*, 616, 91
- Baryshev, Yu.V., Chernin, A.D., & Teerikorpi, P. 2001, *A&A*, 378, 729
- Bellazzini, M., Ferraro, F.R., & Pancino, E. 2001, *ApJ*, 556, 635
- Binggeli, B., Popescu, C.C., & Tammann, G.A. 1993, *A&AS*, 98, 275
- Bono, G., Caputo, F., Castellani, V., Marconi, M., Storm, J., & Degl’Innocenti, S. 2003, *MNRAS*, 344, 1097
- Bottinelli, L., Gouguenheim, L., Paturel, G., & Teerikorpi, P. 1988, *ApJ*, 328, 4
- Branch, D. 1977, in *Supernovae*, ed. D. N. Schramm (Dordrecht: Reidel), 21
- Branch, D. 1998, *ARA&A*, 36, 17
- Branch, D., & Bettis, C. 1978, *AJ*, 83, 224
- Branch, D., & Tammann, G.A. 1992, *ARA&A*, 30, 359
- Byrd, G., Valtonen, M., McCall, M., & Innanen, K. 1994, *AJ*, 107, 2055
- Cadonau, R., Sandage, A., & Tammann, G.A. 1985, in *Supernovae as Distance Indicators, Lecture Notes in Physics 224*, ed. N. Bartel (Berlin: Springer), 151
- Capaccioli, M., Cappellaro, E., della Valle, M., D’Onofrio, M., Rosino, Leonida, & Turatto, M. 1990, *ApJ*, 350, 110

- Carlstrom, J.E., Holder, G.P., & Reese, E.D. 2002, *ARA&A*, 40, 643
- Cassisi, S., & Salaris, M. 1997, *MNRAS*, 285, 593
- Chernin, A.D. 2001, *Physics-Uspekhi*, 44, 1099
- Chernin, A.D., Nagirner, D.I., Starikova, S.V. 2003a, *A&A*, 399, 19
- Chernin, A.D., Teerikorpi, P., Baryshev, Yu. 2003b, *Adv. Space Res.*, 31, 459
- Chernin, A.D., Karachentsev, I.D., Valtonen, M.J., Dolgachev, V.P., Domozhilova, L.M., & Makarov, D.I. 2004, *A&A*, 415, 19
- Chernin, A.D., Karachentsev, I.D., Valtonen, M.J., Dolgachev, V.P., Domozhilova, L.M., & Makarov, D.I. 2005, *astro-ph/0507364*
- Chiosi, C., Wood, P., Bertelli, G., & Bresson, A. 1992, *ApJ*, 387, 320
- Chiosi, C., Wood, P., & Capitanio, N. 1993, *ApJS*, 86, 541
- Christy, R.F. 1966, *ApJ*, 144, 108
- Cowan, J.J., Pfeiffer, B., Kratz, K.-L., Thielemann, F.-K., Sneden, C., Burles, S., Tytler, D., & Beers, T.C. 1999, *ApJ*, 521, 194
- Cox, J.P. 1959, *ApJ*, 130, 296
- Cox, J.P. 1980, *Theory of stellar pulsation*, Princeton Univ. Press, § 10.3
- Da Costa, G.S., & Armandroff, T.E. 1990, *AJ*, 100, 162
- Dall’Ora, M., et al. 2004, *ApJ*, 610, 269
- Dauphas, N. 2005, *Nature*, 435, 1203
- de Vaucouleurs, G., de Vaucouleurs, A., Corwin, H.G., Buta, R.J., Paturel, G., & Fouque, P. 1991, *Third Reference Catalogue of Bright Galaxies*
- Djorgovski, G., & Davis, M. 1987, *ApJ*, 313, 59
- Dressler, A., Lynden-Bell, D., Burstein, D., Davis, R.L., Faber, S.M., Terlevich, R., & Wegner, G. 1987, *ApJ*, 313, 42
- Drinkwater, M.J., Gregg, M.D., Holman, B.A., Brown, M.J.I. 2001, *MNRAS*, 326, 1076
- Ekholm, T., Baryshev, Yu., Teerikorpi, P., Hanski, M.O., & Paturel, G. 2001, *A&A*, 368, 17

- Faber, S.M., & Jackson, R.E. 1976, *ApJ*, 204, 668
- Feast, M.W. 1999, *PASP*, 111, 775
- Federspiel, M. 1999, Ph.D. Thesis, Univ. of Basel
- Federspiel, M., Sandage, A., & Tammann, G.A. 1994, *ApJ*, 430, 29
- Federspiel, M., Tammann, G.A., & Sandage, A. 1998, *ApJ*, 495, 115
- Ferrarese, L., et al. 1997, *ApJ*, 475, 853
- Ferrarese, L., et al. 2000, *ApJS*, 128, 431
- Fiorentino, G., Caputo, F., Marconi, M., & Musella, I. 2002, *ApJ*, 576, 402
- Fitzpatrick, E.L., Ribas, I., Guinan, E.F., DeWarf, L.E., Maloney, F.P., & Massa, D. 2002, *ApJ*, 564, 260
- Fitzpatrick, E.L., Ribas, I., Guinan, E.F., Maloney, F.P., & Claret, A. 2003, *ApJ*, 587, 685
- Fouqué, P., Storm, J., & Gieren, W. 2003, *Lect. Notes Phys.*, 635, 21
- Freedman, W.L., et al. 2001, *ApJ*, 553, 47
- Frogel, J.A., Gregory, B., Kawara, K., Laney, D., Phillips, M.M., Terndrup, D., Vrba, F., & Whitford, A.E. 1987, *ApJ*, 315, 129
- Germany, L.M., Reiss, D.J., Schmidt, B.P., Stubbs, C.W., & Suntzeff, N.B. 2004, *A&A*, 415, 863
- Gibson, B.K., et al. 2000, *ApJ*, 529, 723
- Gieren, W., Storm, J., Barnes, T.G., Fouqué, P., Pietrzynski, G., & Kienzle, F. 2005, *ApJ*, 627, 224
- Graham, J.A., et al. 1999, *ApJ*, 516, 626
- Hamuy, M. 2001, Ph.D. Thesis, Univ. of Arizona
- Hamuy, M., Phillips, M.M., Maza, J., Suntzeff, N.B., Schommer, R.A., & Aviles, R. 1995, *AJ*, 109, 1
- Hamuy, M., Phillips, M.M., Suntzeff, N.B., Schommer, R.A., Maza, J., & Aviles, R. 1996, *AJ*, 112, 2398

- Herrnstein, J.R., et al. 1999, *Nature*, 400, 539
- Hoeflich, P., & Khokhlov, A. 1996, *ApJ*, 457, 500
- Jerjen, H., & Tammann, G.A. 1993, *A&A*, 276, 1
- Jha, S., et al. 1999, *ApJS*, 125, 73
- Jones, M.E., et al. 2005, *MNRAS*, 357, 518
- Karachentsev, I.D. 2005, *AJ*, 129, 178
- Karachentsev, I.D., & Makarov, D.I. 2001, *Astrophys.*, 44, 1
- Karachentsev, I.D., Karachentseva, V.E., Huchtmeier, W.K., & Makarov, D.I. 2004, *AJ*, 127, 2031
- Karachentsev, I.D., et al. 2005, astro-ph/0511648
- Kelson, D.D., et al. 2000, *ApJ*, 529, 768
- Kennicutt, R.C., et al. 1998, *ApJ*, 498, 181
- Kervella, P., Bersier, D., Mourard, D., Nardetto, N., & Coudé du Foresto, V. 2004, *A&A*, 423, 327
- Kochanek, C.S., & Schechter, P.L. 2004, in *Measuring and Modeling the Universe*, ed. W.L. Freedman (Cambridge: Cambridge Univ. Press), 117
- Koopmans, L.V.E., Treu, T., Fassnacht, C.D., Blandford, R.D., & Surpi, G. 2003, *ApJ*, 599, 70
- Kovtyukh, V.V., Wallerstein, G., & Andrievsky, S.M. 2005, *PASP*, 117, 1182
- Kowal, C.T. 1968, *AJ*, 73, 1021
- Kraan-Korteweg, R.C. 1986, *A&AS*, 66, 255
- Lee, M.G., Freedman, W.L., & Madore, B.F. 1993, *ApJ*, 417, 553
- Leibundgut, B. 1988, Ph.D. Thesis, Univ. Basel
- Leibundgut, B. 1991, in *Supernovae*, ed. S.E. Woosley (New York: Springer), 751
- Lynden-Bell, D. 1981, *Observatory*, 101, 111

- Macri, L.M., et al. 1999, *ApJ*, 521, 155
- Madore, B.F., & Freedman, W.L. 1991, *PASP*, 103, 933
- Magain, P. 2005, in *The Light-Time Effect in Astrophysics*, ed. C. Sterken, ASP Conf. Ser. 335, 207
- Makarov, V.V. 2002, *AJ*, 124, 3299
- Marconi, M., Musella, I., & Fiorentino, G. 2005, *ApJ*, 632, 590
- Mould, J.R., et al. 1995, *ApJ*, 449, 413
- Mould, J.R., et al. 2000, *ApJ*, 528, 655
- Nadyozhin, D.K. 2003, *MNRAS*, 346, 97
- Pagel, B.E.J. 2001, in *Cosmic Evolution*, eds. E. Vangioni-Flam, R. Ferlet, & M. Lemoine (New Jersey: World Scientific), 223
- Parodi, B.R., Saha, A., Sandage, A., & Tammann, G.A. 2000, *ApJ*, 540, 634
- Phillips, M.M. 1993, *ApJ*, 413, L105
- Phillips, M.M., Lira, P., Suntzeff, N.B., Schommer, R.A., Hamuy, M., & Maza, J. 1999, *AJ*, 118, 1766
- Pierce, M., & Jacoby, G. 1995, *AJ*, 110, 2885
- Prosser, C.F., et al. 1999, *ApJ*, 525, 80
- Pskovskii, Y.P. 1967, *Sov. Astron.*, 11, 63
- Pskovskii, Y.P. 1984, *Sov. Astron.*, 28, 658
- Rebolo, R., et al. 2004, *MNRAS*, 353, 747
- Reindl, B., Tammann, G.A., Sandage, A., & Saha, A. 2005, *ApJ*, 624, 532 (Paper III)
- Ribas, I., Jordi, C., Vilardell, F., Fritzpatrick, E.L., Hilditch, R.W., & Guinan, E.F. 2005, *ApJ*, 635, L37
- Richter, O.-G., Tammann, G.A., & Huchtmeier, W.K. 1987, *A&A*, 171, 33
- Richtler, T., & Drenkhahn, G. 1999, in *Cosmology and Astrophysics*, eds. W. Kundt W. & C. van de Bruck, *asto-ph/9909117*

- Riess, A.G., Press, W.H., & Kirshner, R.P. 1995, ApJ, 438, L17
- Riess, A.G., et al. 2005, ApJ, 627, 579
- Saha, A., Labhardt, L., Schwengeler, H., Macchetto, F.D., Panagia, N., Sandage, A. , & Tammann, G.A. 1994, ApJ, 425, 14
- Saha, A., Sandage, A., Labhardt, L., Schwengeler, H., Tammann, G.A., Panagia, N., & Macchetto, F.D. 1995, ApJ, 438, 8
- Saha, A., Sandage, A., Labhardt, L., Tammann, G.A., Macchetto, F.D., & Panagia, N. 1996a, ApJ, 466, 55
- Saha, A., Sandage, A., Labhardt, L., Tammann, G.A., Macchetto, F.D., & Panagia, N. 1996b, ApJS, 107, 693
- Saha, A., Sandage, A., Labhardt, L., Tammann, G.A., Macchetto, F.D., & Panagia, N. 1997, ApJ, 486, 1
- Saha, A., Sandage, A., Tammann, G.A., Labhardt, L., Macchetto, F.D., & Panagia, N. 1999, ApJ, 522, 802
- Saha, A., Sandage, A., Tammann, G.A., Dolphin, A.E., Christensen, J., Panagia, N., & Macchetto, F.D. 2001, ApJ, 562, 314
- Saha, A., Thim, F., Tammann, G.A., Reindl, B., & Sandage, A. 2006, ApJS, 165, 108, (Paper IV)
- Saha, P., & Williams, L.L.R. 2003, AJ, 125, 2769
- Saha, P., Coles, J., Macciò, A.V., & Williams, L.L.R. 2006, astro-ph/0607240
- Sakai, S., et al. 2000, ApJ, 529, 698
- Sakai, S., Ferrarese, L., Kennicutt, R.C., & Saha, A. 2004, ApJ, 608, 42
- Sandage, A. 1986, ApJ, 307, 1
- Sandage, A. 1994, ApJ, 430, 1
- Sandage, A. 1996, AJ, 111, 1
- Sandage, A. 1999, ApJ, 527, 479

- Sandage, A., & Bedke, J. 1988, Atlas of galaxies useful for measuring the cosmological distance scale (Washington: NASA), 10
- Sandage, A., Bell, R.A., & Tripicco, M.J. 1999, ApJ, 522, 250
- Sandage, A., & Tammann, G.A. 1982, ApJ, 256, 339
- Sandage, A., & Tammann, G.A. 1990, ApJ, 365, 1
- Sandage, A., & Tammann, G.A. 2006a, ARA&A, 44, in press
- Sandage, A., & Tammann, G.A. 2006b, ApJ, submitted
- Sandage, A., Tammann, G.A., & Hardy, E. 1972, ApJ, 172, 253
- Sandage, A., Tammann, G.A., & Reindl, B. 2004, A&A, 424, 43 (Paper II)
- Schaefer, B.E. 1995, ApJ, 449, L9
- Schaefer, B.E. 1996a, AJ, 111, 1668
- Schaefer, B.E. 1996b, ApJ, 460, L19
- Schaefer, B.E. 1998, ApJ, 509, 80
- Schlegel, D., Finkbeiner, D., & Davis, M. 1998, ApJ, 500, 525
- Schmidt, B.P., Kirshner, R.P., Eastman, R.G., Phillips, M.M., Suntzeff, N.B., Hamuy, M., Maza, J., & Avilés, R. 1994, ApJ, 432, 42
- Silbermann, N.A., et al. 1999, ApJ, 515, 1
- Snedden, C., et al. 2003, ApJ, 591, 936
- Spergel, D.N., et al. 2003, ApJS, 148, 175
- Spergel, D.N., et al. 2006, astro-ph/0603449
- Suntzeff, N.B., et al. 1999, ApJ, 500, 525
- Tammann, G.A. 1979, in Scientific Research with the Space Telescope, IAU Coll. 45, 263
- Tammann, G.A. 1982, in Supernovae: A Survey of Current Research, eds. M.J. Rees & R.J. Stoneham (Dordrecht: Reidel), 371

- Tammann, G.A., Reindl, B., Thim, F., Saha, A., & Sandage, A. 2002, in *A New Era in Cosmology*, eds. T. Shanks, & N. Metcalfe, ASP Conf. Ser. 283, 258
- Tammann, G.A., & Sandage, A. 1985, *ApJ*, 294, 81
- Tammann, G.A., & Sandage, A. 1995, *ApJ*, 452, 16
- Tammann, G.A., Sandage, A., & Reindl, B. 2003, *A&A*, 404, 423 (Paper I)
- Tanvir, N.R., Hendry, M.A., Watkins, A., Kanbur, S.M., Berdnikov, L.N., & Ngeow, C.-C. 2005, *MNRAS*, 363, 749
- Teerikorpi, P. 1987, *A&A*, 173, 39
- Teerikorpi, P. 1990, *A&A*, 234, 1
- Teerikorpi, P. 1997, *ARA&A*, 35, 101
- Teerikorpi, P., Chernin, A.D., & Baryshev, Yu.V. 2005, *A&A*, 440, 791
- Thim, F., Tammann, G.A., Saha, A., Dolphin, A., Sandage, A., Tolstoy, E., & Labhardt, L. 2003, *ApJ*, 590, 256
- Tonry, J.L., Blakeslee, J.P., Ajhar, E.A., & Dressler, A. 2000, *ApJ*, 530, 625
- Tonry, J.L., & Schneider, D. 1988, *AJ*, 96, 807
- Tripp, R., & Branch, D. 1999, *ApJ*, 525, 209
- Truran, J.W., Burles, S., Cowan, J.J., Sneden, C. 2001, in *Astrophysical Ages and Times Scales*, eds. T. von Hippel, C. Simpson, & N. Manset, ASP Conf. Ser. 245, 226
- Tsvetkov, D.Y. 1983, *Perem. Zvezdy*, 22, 39
- Tuggle, R.S., & Iben, I. 1972, *ApJ*, 178, 455
- Tully, R.B., & Fisher, J.R. 1977, *A&A*, 54, 661
- Udalski, A., Szymanski, M., Kubiak, M., Pietrzynski, G., Soszynski, I., Wozniak, P., & Zebrun, K. 1999, *AcA*, 49, 201
- Udomprasert, P.S., Mason, B.S., Readhead, A.C.S., & Pearson, T.J. 2004, *ApJ*, 615, 63
- van Albada, T.S., & Baker, N. 1971, *ApJ*, 169, 311
- VandenBerg, D.A., Richard, O., Michaud, G., & Richer, J. 2002, *ApJ*, 571, 487

van den Bergh, S. 1960a, ApJ, 131, 215

van den Bergh, S. 1960b, ApJ, 131, 558

Vollmer, B. 2003, A&A, 398, 525

Westin, J., Sneden, C., Gustafsson, B., & Cowan, J.J. 2000, ApJ, 530, 783

Wang, X., Wang, L., Pain, R., Zhou, X., & Li, Z. 2006, ApJ, 645, 488

Yahil, A., Tammann, G.A., & Sandage, A. 1977, ApJ, 217, 903

Yahil, A., Sandage, A., & Tammann, G.A. 1980, in Physical Cosmology, eds. E. Balian, J. Audouze, & D.N. Schramm (Amsterdam: North-Holland), 127

York, T., Jackson, N., Browne, I.W.A., Wucknitz, O., & Skelton, J.E. 2005, MNRAS, 357, 124

Table 1. Parameters of Galaxies with SNeIa and Cepheid Distances.

SN (1)	Galaxy (2)	v_0 (3)	v_{220} (4)	$[\text{O}/\text{H}]_{\text{old}}$ (5)	$[\text{O}/\text{H}]_{\text{Sakai}}$ (6)	N (7)	$\langle \log P \rangle$ (8)	$\mu^0(\text{Gal})$ (9)	$\mu^0(\text{LMC})$ (10)	$\mu_Z^0(\text{M/F})$ (11)	μ_Z^0 (12)	$\epsilon(\mu_Z^0)$ (13)
1937C	IC 4182	342	303	8.40	8.20	13	1.387	28.51	28.32	28.25	28.21	0.10
1960F	NGC 4496A	1573	1152	8.77	8.53	39	1.514	31.24	30.99	31.17	31.18	0.10
1972E	NGC 5253	156	170	8.15	8.15	5	1.029	28.11	28.09	27.89	28.05	0.27
1974G	NGC 4414	691	1137	9.20	8.77	10	1.526	31.55	31.29	31.63	31.65	0.17
1981B	NGC 4536	1645	(1152)	8.85	8.58	27	1.566	31.26	30.98	31.20	31.24	0.10
1989B	NGC 3627	597	427	9.25	8.80	22	1.452	30.41	30.19	30.53	30.50	0.10
1990N	NGC 4639	901	1152	9.00	8.67	12	1.552	32.13	31.86	32.13	32.20	0.10
1991T	NGC 4527	1575	(1152)	8.75	8.52	19	1.498	30.84	30.59	30.76	30.76	0.20
1994ae	NGC 3370	1169	1611	8.80	8.55	64	1.548	32.42	32.14	32.35	32.37	0.10
1998aq	NGC 3982	1202	1510	8.75	8.52	15	1.502	31.94	31.69	31.86	31.87	0.15
1998bu	NGC 3368	760	708	9.20	8.77	7	1.467	30.25	30.02	30.34	30.34	0.11
1999by	NGC 2841	716	895	8.80	8.55	18	1.445	30.79	30.57	30.74	30.75	0.10

Table 2. Parameters of SNeIa with Cepheid Distances.

SN (1)	Δm_{15} (2)	E_{Gal} (3)	E_{host} (4)	$(B-V)$ (5)	$(V-I)$ (6)	m_B^{corr} (7)	m_V^{corr} (8)	m_I^{corr} (9)
1937C	0.85	0.014	-0.022	-0.012	...	8.97 (09)	8.99 (11)	...
1960F	0.87	0.025	0.099	-0.034	...	11.28 (15)	11.31 (20)	...
1972E	1.05	0.056	-0.050	-0.006	-0.316	8.46 (14)	8.49 (15)	8.77 (19)
1974G	1.11	0.019	0.161	+0.000	...	11.79 (05)	11.82 (05)	...
1981B	1.13	0.018	0.037	+0.005	...	11.79 (05)	11.82 (05)	...
1989B	1.31	0.032	0.311	+0.007	-0.162	10.93 (05)	10.95 (05)	11.11 (05)
1990N	1.05	0.026	0.034	-0.040	-0.298	12.56 (05)	12.59 (05)	12.89 (05)
1991T	0.94	0.022	0.199	-0.031	-0.411	10.98 (05)	11.00 (05)	11.39 (05)
1994ae*	0.90	0.030	0.034	-0.064	-0.294	12.98 (05)	13.01 (05)	13.31 (05)
1998aq*	1.05	0.014	-0.048	-0.066	-0.214	12.54 (05)	12.56 (05)	12.82 (05)
1998bu	1.15	0.025	0.279	+0.056	-0.191	11.01 (05)	11.04 (05)	11.14 (05)
1999by	1.90	0.016	...	+0.494	+0.219	13.59 (05)	13.10 (05)	12.88 (05)

Note. — * The photometry is from Riess et al. (2005) and reduced as in Paper III.

Table 3. Absolute Magnitudes of SNe Ia and Solutions for H_0 .

SN (1)	from Gal. $P-L$			from LMC $P-L$			from M/F $P-L$			from μ_Z^0		
	M_B (2)	M_V (3)	M_I (4)	M_B (5)	M_V (6)	M_I (7)	M_B (8)	M_V (9)	M_I (10)	M_B (11)	M_V (12)	M_I (13)
1937C	-19.54 (13)	-19.52 (15)	...	-19.35 (13)	-19.33 (15)	...	-19.28 (13)	-19.26 (15)	...	-19.24 (13)	-19.22 (15)	...
1960F	-19.96 (18)	-19.93 (22)	...	-19.71 (18)	-19.68 (22)	...	-19.89 (18)	-19.86 (22)	...	-19.90 (18)	-19.87 (22)	...
1972E	-19.65 (30)	-19.62 (31)	-19.34 (33)	-19.63 (30)	-19.60 (31)	-19.32 (33)	-19.43 (30)	-19.40 (31)	-19.12 (33)	-19.59 (30)	-19.56 (31)	-19.28 (33)
1974G	-19.76 (18)	-19.73 (18)	...	-19.50 (18)	-19.47 (18)	...	-19.84 (18)	-19.81 (18)	...	-19.86 (18)	-19.83 (18)	...
1981B	-19.47 (11)	-19.44 (11)	...	-19.19 (11)	-19.16 (11)	...	-19.41 (11)	-19.38 (11)	...	-19.45 (11)	-19.42 (11)	...
1989B	-19.48 (11)	-19.46 (11)	-19.30 (11)	-19.26 (11)	-19.24 (11)	-19.08 (11)	-19.60 (11)	-19.58 (11)	-19.42 (11)	-19.57 (11)	-19.55 (11)	-19.39 (11)
1990N	-19.57 (11)	-19.54 (11)	-19.24 (11)	-19.30 (11)	-19.27 (11)	-18.97 (11)	-19.57 (11)	-19.54 (11)	-19.24 (11)	-19.64 (11)	-19.61 (11)	-19.31 (11)
1994ae	-19.44 (11)	-19.41 (11)	-19.11 (11)	-19.16 (11)	-19.13 (01)	-18.83 (11)	-19.37 (11)	-19.34 (11)	-19.04 (01)	-19.39 (11)	-19.36 (11)	-19.06 (11)
1998aq	-19.40 (16)	-19.38 (16)	-19.12 (16)	-19.15 (16)	-19.13 (16)	-18.87 (16)	-19.32 (16)	-19.30 (16)	-19.04 (16)	-19.33 (16)	-19.31 (16)	-19.05 (16)
1998bu	-19.24 (12)	-19.21 (12)	-19.11 (12)	-19.01 (12)	-18.98 (12)	-18.88 (12)	-19.33 (12)	-19.30 (12)	-19.20 (12)	-19.33 (12)	-19.30 (12)	-19.20 (12)
mean	-19.55 (06)	-19.52 (06)	-19.20 (04)	-19.33 (07)	-19.30 (07)	-18.99 (08)	-19.50 (07)	-19.48 (07)	-19.18 (06)	-19.53 (07)	-19.50 (07)	-19.22 (06)
weighted	-19.50 (04)	-19.47 (04)	-19.19 (05)	-19.26 (04)	-19.22 (04)	-18.94 (05)	-19.48 (04)	-19.45 (04)	-19.20 (05)	-19.49 (04)	-19.46 (04)	-19.22 (05)
H_0 (mean)	60.7 (1.7)	60.8 (1.7)	62.7 (1.2)	67.1 (2.2)	67.3 (2.2)	69.0 (2.6)	61.8 (2.0)	61.9 (2.0)	63.2 (1.8)	61.2 (2.0)	61.4 (2.0)	62.1 (1.4)
H_0 (weighted)	62.1 (1.2)	62.2 (1.2)	63.0 (1.5)	69.3 (1.3)	69.8 (1.3)	70.6 (1.6)	62.7 (1.2)	62.8 (1.2)	62.7 (1.5)	62.4 (1.2)	62.5 (1.2)	62.1 (1.2)
non-standard spectra												
1991T	-19.86 (21)	-19.84 (21)	-19.45 (21)	-19.61 (21)	-19.59 (21)	-19.20 (21)	-19.78 (21)	-19.76 (21)	-19.37 (21)	-19.78 (21)	-19.76 (21)	-19.37 (21)
1999by	-17.20 (11)	-17.69 (11)	-17.91 (11)	-16.98 (11)	-17.47 (11)	-17.69 (11)	-17.15 (11)	-17.64 (11)	-17.86 (11)	-17.16 (11)	-17.65 (11)	-17.87 (11)

Note. — H_0 from $c_B = 0.693 \pm 0.004$, $c_V = 0.688 \pm 0.004$, $c_I = 0.637 \pm 0.004$ (from Paper III) and $\log H_0 = 0.2 \cdot M_\lambda + c_\lambda + 5$

Table 4. Weighted, Metallicity-Corrected Mean Absolute Magnitudes of SNe Ia. The Error of the Mean is 0.04 mag for All Entries.

	M_B	M_V	M_I
1) from $\mu^0(\text{Gal})$	-19.50	-19.47	-19.19
2) from $\mu_Z^0(\text{LMC})$	-19.36	-19.32	-19.07
3) from $\mu_Z^0(\text{M/F})$	-19.48	-19.45	-19.20
4) from μ_Z^0 (Paper IV)	-19.49	-19.46	-19.22
mean of 1) – 4)	-19.46	-19.43	-19.17
mean of 1), 3), & 4)	-19.49	-19.46	-19.20

Table 5. Mean Properties of Calibrating and Distant SNe Ia.

	N	$\langle(B-V)^{\text{corr}}\rangle$	$\langle(V-I)^{\text{corr}}\rangle$	$\langle E(B-V)_{\text{host}}\rangle$	$\langle\Delta m_{15}\rangle$	$\langle\text{Host Galaxy Type}\rangle$
Calibrators	10	−0.024	−0.235	0.084	1.05	4.0
Distant SNe Ia	62	−0.024	−0.251	0.057	1.22	1.5

Table 6. Overview of H_0 Values from SNe Ia.

authors	cal SNe	dist SNe	H_0
Sandage & Tammann 1982	2	16	50 ± 7
Capaccioli et al. 1990	10	5	70 ± 15
Saha et al. 1994	1	34	52 ± 9
Riess et al. 1995	1	13	67 ± 7
Saha et al. 1995	3	34	52 ± 8
Tammann & Sandage 1995	3	39	56.5 ± 4
Mould et al. 1995	6	21	71 ± 7
Saha et al. 1996a	4	39	56.5 ± 3
Hamuy et al. 1996	4	29	$63.1 \pm 3.4 \pm 2.9$
Hoeflich & Khokhlov 1996	theory	26	67 ± 9
Saha et al. 1997	7	56	58 ± 8
Saha et al. 1999	9	35	60 ± 2
Tripp & Branch 1999	6/10	26/29	62.9 ± 4.7
Suntzeff et al. 1999	8	40	$63.9 \pm 2.2 \pm 3.5$
Phillips et al. 1999	6	40	$63.3 \pm 2.2 \pm 3.5$
Jha et al. 1999	4	42	$64.4 \pm 6.6 \pm 5.4$
Richtler & Drenkhahn 1999	4	26	72 ± 4
Gibson et al. 2000	6	40	$68 \pm 2 \pm 5$
Parodi et al. 2000	8	35	58.5 ± 4.0
Freedman et al. 2001	6	36	$72 \pm 2 \pm 6$
Saha et al. 2001	9	35	$58.7 \pm 2 \pm 6$
Altavilla et al. 2004	9	18-46	$68 - 74$
Riess et al. 2005	4	68	73 ± 4
Wang et al. 2006	11	73	72 ± 4
Present Paper	10	62	$62.3 \pm 1.3 \pm 5.0$

Table 7. Distance of the Virgo and Fornax Cluster from Cepheids, SNe Ia, and 21cm-line Widths.

	Object	Virgo μ_Z^0	Object	Fornax μ_Z^0
Cepheids	N4321	31.18	N1326A	31.17
	N4535	31.25	N1365	31.46
	N4548	30.99	N1425	31.96
	N4639	32.20		
SNe Ia	1984A	31.15	1980N	31.67
	1990N	32.05	1981D	31.30
	1994D	31.30	1992A	31.82
21cm-line widths	31.58			
	$\langle \mu^0 \rangle$	31.47 ± 0.16		31.56 ± 0.13
	$\langle \mu_0^0 \rangle$	31.51 ± 0.16		31.56 ± 0.13
	$\langle v_\odot \rangle$	1050 ± 35^1		1493 ± 36^2
	$\langle v_0 \rangle$	932		1403
	$\langle v_{00} \rangle$	932		1403
	$\langle v_{220} \rangle$	$1152 (\pm 35)$		1371
	v_{cosmic}	1175 ± 30^3		...
	H_0	58.1 ± 4.6		66.8 ± 4.0

¹)Binggeli et al. (1993)

²)Drinkwater et al. (2001)

³)Jerjen & Tammann (1993). The value is inferred from the distance ratios between the Virgo cluster and more remote clusters whose CMB-corrected velocities are taken to define the cosmic expansion field.

Note. — The Cepheid distances have been determined in Paper IV (Table A1) from the original Cepheid data by Ferrarese et al. (1997, for NGC 4321), Macri et al. (1999, for NGC 4535), Graham et al. (1999, for NGC 4548), Saha et al. (1997, for NGC 4639), Prosser et al. (1999, for NGC 1326A), Silbermann et al. (1999, for NGC 1365), and Mould et al. (2000, for NGC 1425).

Table 8. Parameters of the Three Nearest Galaxy Groups.

Group (1)	N (2)	$\langle D \rangle$ (3)	$\langle D_0 \rangle$ (4)	$\langle v_{\odot} \rangle$ (5)	$\langle v_0 \rangle$ (6)	$\langle v_{00} \rangle$ (7)	$\langle v_{220} \rangle$ (8)	H_i (9)	Δv_{Hubble} (10)
M 81	29	3.69	3.50	51±20	211	213	234	66.8±6	23
Cen A	20	3.75	4.29	536±26	261	262	288	67.1±6	29
IC 342	7	3.36	2.94	12±18	256	258	290	98.5±6	113